ERDC/GSL TR-21-15

US Army Corps
of Engineers®
Engineer Research and
Development Center

ERDC
ENGINEER RESEARCH & DEVELOPMENT CENTER

SBIR Phase II Sub-award Report Phase 2B

Performance of Active Porcelain Enamel Coated Fibers for Fiber-Reinforced Concrete

The Performance of Active Porcelain Enamel Coatings for Fiber-Reinforced Concrete and Fiber Tests at the University of Louisville

Charles A. Weiss Jr., William M. McGinley, Bradford P. Songer,
Madeline A. Kuchinski, and Frank A. Kuchinski

May 2021

Geotechnical and Structures Laboratory

The U.S. Army Engineer Research and Development Center (ERDC) solves the nation's toughest engineering and environmental challenges. ERDC develops innovative solutions in civil and military engineering, geospatial sciences, water resources, and environmental sciences for the Army, the Department of Defense, civilian agencies, and our nation's public good. Find out more at www.erdc.usace.army.mil.

To search for other technical reports published by ERDC, visit the ERDC online library at https://erdclibrary.on.worldcat.org/discovery.

ERDC/GSL TR-21-15
May 2021

Performance of Active Porcelain Enamel Coated Fibers for Fiber-Reinforced Concrete

The Performance of Active Porcelain Enamel Coatings for Fiber-Reinforced Concrete and Fiber Tests at the University of Louisville

Charles A. Weiss Jr. and Bradford P. Songer

Geotechnical and Structures Laboratory
U.S. Army Engineer Research and Development Center
3909 Halls Ferry Road
Vicksburg, MS 39180

William M. McGinley

Department of Civil and Environmental Engineering
University of Louisville
Louisville, KY 40292
for Ceramics, Composites and Coatings Inc.

Madeline A. Kuchinski and Frank A. Kuchinski

Ceramics, Composites and Coatings Inc.
1829 William Penn Way
Lancaster, PA 17601

Final report

Prepared for U.S. Army Corps of Engineers
Washington, DC 20314-1000

Under Small Business Innovation Research (SBIR) under Solicitation Number A14-090, “Highly Flexible Chopped Fiber Coating Apparatus,” contract W912HZ-16-C-0015

Abstract

A patented active porcelain enamel coating improves both the bond between the concrete and steel reinforcement as well as its corrosion resistance. A Small Business Innovation Research (SBIR) program to develop a commercial method for production of porcelain-coated fibers was developed in 2015. Market potential of this technology with its steel/concrete bond improvements and corrosion protection suggests that it can compete with other fiber reinforcing systems, with improvements in performance, durability, and cost, especially as compared to smooth fibers incorporated into concrete slabs and beams.

Preliminary testing in a Phase 1 SBIR investigation indicated that active ceramic coatings on small diameter wire significantly improved the bond between the wires and the concrete to the point that the wires achieved yield before pullout without affecting the strength of the wire.

As part of an SBIR Phase 2 effort, the University of Louisville under contract for Ceramics, Composites and Coatings Inc., proposed an investigation to evaluate active enamel-coated steel fibers in typical concrete applications and in masonry grouts in both tension and compression.

Evaluation of the effect of the incorporation of coated fibers into Ultra-High Performance Concrete (UHPC) was examined using flexural and compressive strength testing as well as through nanoindentation.

Contents

Figures and Tables

Figures

Tables

Preface

This study was prepared for the U.S. Army Corps of Engineers and conducted for the Small Business Innovation Research (SBIR) Program under Solicitation Number A14-090, "Highly Flexible Chopped Fiber Coating Apparatus," contract W912HZ-16-C-0015. The technical monitor was Dr. Charles A. Weiss Jr. A portion of the research was performed by University of Louisville, under subcontract to Small Business Award recipient Ceramics, Composites and Coatings Inc.

The work was performed by the Research Group (GMR) and Concrete and Materials Branch (GMC) of the Engineering Systems and Materials Division Branch (GM), Geotechnical and Structures Laboratory (GSL), U.S. Army Engineer Research and Development Center (ERDC). At the time of publication, Dr. Jameson Shannon was Chief, GMC; Mr. Justin S. Strickler was Chief, GM; and Ms. Pamela G. Kinnebrew, GZ, was the Lead Technical Director for Military Engineering. The Deputy Director of ERDC-GSL was Mr. Charles W. Ertle II, and the Director was Mr. Bartley P. Durst.

COL Teresa A. Schlosser was the Commander of ERDC, and Dr. David W. Pittman was the Director.

1 Introduction

A patented active porcelain enamel coating, when applied to reinforcing steel, has been shown to improve both the corrosion resistance of the reinforcement and the bond between the steel and the concrete material. Market potential of this technology with both steel/concrete bond improvements and corrosion protection suggests that it can compete with other fiber-reinforcing systems, with improvements in performance, durability, and cost, especially as compared to smooth fibers incorporated into concrete slabs and beams. Significant improvement in slab cracking, durability, and strength can be realized as well.

Preliminary testing in a Phase 1 Small Business Innovation Research (SBIR) investigation indicated that active ceramic coatings could be applied to small diameter wire, and these coatings significantly improved the bond between the wires and the concrete to the point that the wires achieved yield before pullout. This effect was achieved without deleteriously affecting the strength of the wire. These preliminary tests also showed that relatively large volumes of coated fibers could be incorporated into concrete mixtures without a significant impact on plastic mixture workability.

As part of an SBIR Phase 2 effort (in a subcontract to Ceramics, Composites and Coatings Inc. [3CInc]), the University of Louisville proposed an investigation to evaluate the active enamel-coated steel fibers in typical concrete applications. During this SBIR Phase 2 investigation, fiber length and loading optimization were to be addressed, as was the development/evaluation of a variety of trial steel fiber configurations with active porcelain enamel coatings. In addition, applications of coated fiber in masonry wall grout, as well as their impact on the response of fiber-reinforced concrete in compression, were to be evaluated. The following experimental research investigation was conducted under this Phase 2 testing, including the investigation of coated fiber application in ultra-high performing concrete (UHPC) conducted by the U. S. Army Engineer Research and Development Center (ERDC).

2 Testing Program

Based on analyses of previous steel fiber-reinforced concrete research (Lui 2017), it appears that the best performance (strength) of fiber-reinforced concrete may be generally obtained by using fibers that are at least 1.5 in. in length and have length-to-diameter ratios of approximately 20, with higher ratios generally producing higher strengths with better dispersions. Based on these results, the testing program proposed to evaluate three fiber diameters: 0.080 in., 0.047 in., and 0.029 in. Use of a 1.5-in.-long fiber results in length-to-diameter ratios of 18.8, 31.9, and 51.7, respectively. Two-inch-long fibers may give better performance, as they will increase the length-to-diameter ratios, but this additional length was expected to negatively impact the concrete mixture workability; therefore, fiber length was restricted to 1.5 in. for this study.

The 0.029-in.-diam fiber was more difficult to coat in substantial volumes with the current process; therefore, only a limited number of tests were conducted with the 0.029-in.-diam. fiber. The 0.047-in.-diam fiber was identified by 3CInc as the thinnest fiber that could be easily coated with the active enamel coating using current production processes in greater than 100-lb quantities. For the fixed 1.5-in. length and three fiber diameters, a number of tests were conducted on both uncoated and coated fibers as described below.

2.1 Beam tests

A series of three standard (6-in. x 6-in. x 21-in.) ASTM C78 (2014) beam specimens was fabricated for a variety of fiber and concrete beam configurations. In addition to a control beam set with no fibers, beam specimens with a total of four different mixing configurations were fabricated with a number of coated and uncoated fiber loadings. Table 1 shows a summary of the beam configurations.

Table 1. Beam specimen configurations (three replicates for each configuration).

Beam	Fiber Type	Fiber Volume (%)
No Fiber	None - Control	
Uncoated Fiber	Uncoated steel fiber; Diam = 0.08 in., 1.5 in. long.	3
Uncoated Fiber Mix	Uncoated steel fiber; Diam = 0.08 and 0.047 in., 1.5 in. long.	1.5 + 1.5
Coated Fiber	Coated steel fiber; Diam = 0.08 in., 1.5 in. long	3
Coated Fiber Mix	Coated steel fiber; Diam = 0.08 and 0.047 in., 1.5 in. long.	1.5 + 1.5

For each beam configuration, three replicates were cast using a single batch of concrete. The concrete was mixed for 5 min after the addition of water. Three compression cylinders were taken from select mixtures before fibers were added. After cylinders were taken, the mixer was restarted and the fibers (Figure 1) were gradually added to the mixer over a 2- to 3-min period (Figure 2). The fiber concrete was mixed a minimum of 5 min after the first addition of fibers. Slightly longer mixing times (up to 30 sec longer) were used for higher fiber loadings to ensure all aggregates and fibers were coated with paste and reasonably well-distributed. The concrete was then loaded into the beam forms in two equal lifts and vibrated at each lift to consolidate the concrete and fibers (Figure 3). The forms were then troweled to the required finish (Figure 4). All loading configurations of fiber concrete were reasonably easy to trowel and finish.

Figure 1. Coated steel fibers.

Figure 2. Concrete after coated fibers added (3% loading).

Figure 3. Fiber-reinforced concrete added to the beam mold and vibrated (3% loading).

Figure 4. Finished fiber-reinforced concrete beams (3% loading).

For each batch, three concrete compression cylinders were also cast and tested for compressive strength by using the procedures in ASTM C39 (2015) over the period of beam testing. After casting, all beams were then stripped after 24 hr and placed in a curing room at 95-100% relative humidity and 72-76°F. Beams were then removed and tested after curing

for at least 14 days. High-early-strength cement (Type III) was used in mixture proportions, and compression cylinders were tested to ensure that the concrete strength was approximately equal to the 5,000-psi design strength before flexural testing. This process allowed for more expedited curing and testing of each mixture proportion.

The three concrete cylinders for each concrete batch were tested for compressive strength by using the procedures in ASTM C39 (2015) at the same time that the beam tests were conducted. These tests were used to characterize the concrete mixture.

Third point loading flexural tests were conducted on all the beam specimens using the configuration shown in Figures 5 and 6. Both load and midspan deformations were monitored. The beam tests were conducted by using the procedures described in ASTM C78 (2014) and ASTM C1399 (2016b) in an effort to determine the cracking load and the residual strength that the fibers impart to the beams. All fiber-reinforced beams were tested by using the steel plate under the beam as required in ASTM C1399. This plate was removed after cracking, and the beams were reloaded as described in ASTM C1399.

Figure 5. Beam test configuration (modified from ASTM C78 [2014]).

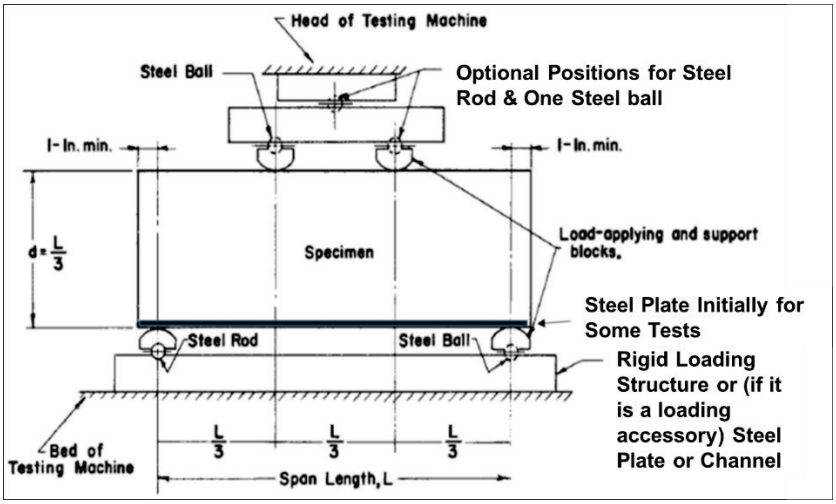

Figure 6. Beam specimen just prior to testing with plate.

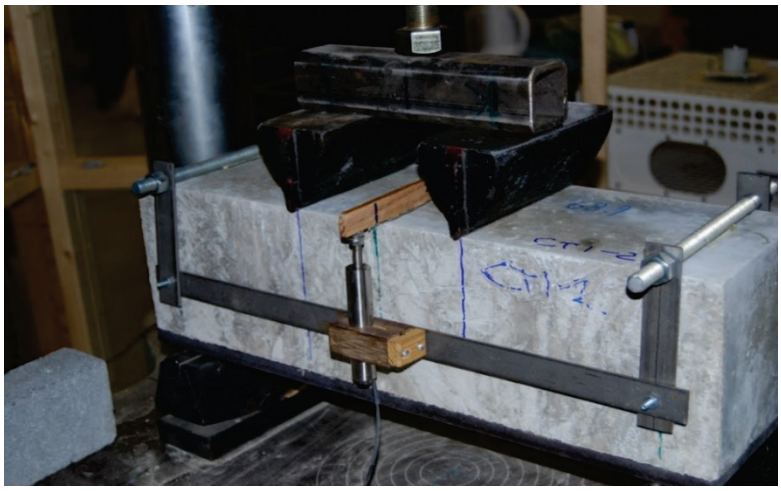

2.2 Compression tests

The second part of the testing program included compression tests of concrete cylinders. Three 4-in. x 8-in. concrete cylinder specimens were fabricated for a variety of fiber type and volume configurations. The authors recognize that the cylinder size used was non-standard: because the maximum fiber size was 1.5 in., standard cylinder diameter size should have been at least 4.5 in. In addition to a control set with no fibers, nine different mixing configurations were addressed using a number of coated and uncoated fiber loadings. Table 2 shows a summary of these configurations.

Table 2. Concrete cylinder specimen configuration (three replicates for each configuration).

Set No.	Fiber Type	Fiber Volume (%)
1	None – Control	NA
2	Coated steel fiber; Diam = 0.047 in., Length = 1.5 in.	1
3	Coated steel fiber; Diam = 0.047 in., Length = 1.5 in.	3
4	Coated steel fiber; Diam = 0.029 in., Length = 1.5 in.	1
5	Coated steel fiber; Diam = 0.029 in., Length = 1.5 in.	3
6	Uncoated steel fiber; Diam = 0.029 in., Length = 1.5 in.	1
7	Uncoated steel fiber; Diam = 0.029 in., Length = 1.5 in.	3
8	Coated steel fiber; Diam = 0.080 in., Length = 1.5 in.	3
9	Uncoated steel fiber; Diam = 0.080 in., Length = 1.5 in.	3
10	Uncoated steel fiber; Diam = 0.047 in., Length = 1.5 in.	1

For each cylinder configuration, three replicates were cast using a single batch of concrete. Following the same mixing procedures as for the beam tests, the concrete was mixed for 5 min after the addition of water. After the initial mixing, the fibers (Figure 7) were gradually added to the mixer over a 2- to 3-min period. The fiber concrete was mixed a minimum of 5 min after the first addition of fibers to allow for adequate coating and dispersion of fibers. The concrete was then loaded into the cylinder forms in two equal lifts and vibrated (at each lift) to consolidate the concrete and the fibers. The forms were then finished. Most of the loading configurations of fiber concrete were easy to trowel and finish with few exceptions (Figure 8).

Figure 7. Contrast between (left) coated and (right) uncoated 0.029-in.-diam fibers.

Figure 8. Rough cylinder finishing (0.029-in.-diam, uncoated fibers at 3% by volume).

Once all the cylinders were cast, they were left untouched for 24 hr in ambient laboratory conditions. They were then stripped and placed in a curing room at a relative humidity of 95-100% and a temperature of 72-76°F. After an additional 24 hr, the cylinders were removed from the curing room and capped with molten sulfur (Figure 9). The cylinders were then put back into the curing room. After 14±3 days curing time, each cylinder was tested for compressive strength and strain response using the procedures in ASTM C39 (2015; Figure 10).

Figure 9. Capped cylinders.

Figure 10. Compression cylinder and strain sensor prior to testing.

2.3 Masonry wallet tests

The final tests conducted in this phase of the testing program consisted of pullout tests on rebar cast into masonry wallets. Three wallet specimens were fabricated for three different grout/fiber configurations. An additional set of wallets was also fabricated using grout with no fibers as a control. The fiber volume was limited to 2% of the total volume based on the concrete mixing performance of the 3% mixes in the compression tests. A fine grout mix of approximately one part cement to three parts masonry sand was used in construction. Table 3 shows details on the grout/fiber mix configurations for each wallet set.

Table 3. Masonry wallet specimen configurations (three replicates for each configuration).

Wallet Set No.	Fiber Type	Fiber Volume (%)
1	None - Control	0
2	Coated steel fiber; Diam = 0.029 in., Length = 1.5 in.	1
3	Coated steel fiber; Diam = 0.047 in., Length = 1.5 in.	1
4	Coated steel fiber; Diam = 0.047 in., Length = 1.5 in.	2

Twelve (three per set) 4-ft x 4-ft x 8-in. (nominal) masonry wallets were built in accordance with typical masonry practice using trained masons. ASTM C90 (2016a) 8-in. hollow concrete masonry units and type S masonry cement mortar were used. Two No. 7 rebars were placed together to create a vertical lap splice at two locations in masonry wallets approximately 15 in. apart, as shown in Figure 11. The lap splices were formed in a single grouted cell, and only the cells that had bars were grouted (to represent the worst conditions in the field). These No. 7 Grade 60 steel reinforcing bars had a lap splice of 32 in., well below the 52-in. lap splice required by the masonry design code for a specified masonry strength (f'_m) of 2,000 psi. Based on the commentary to the code, a 52-in. splice would allow at least 1.25% of the specified yield strength of the 60-ksi rebar to be developed. The 32-in. lap splice was expected to fall below the yield strength of the bar.

Figure 11. Wallet specimen.

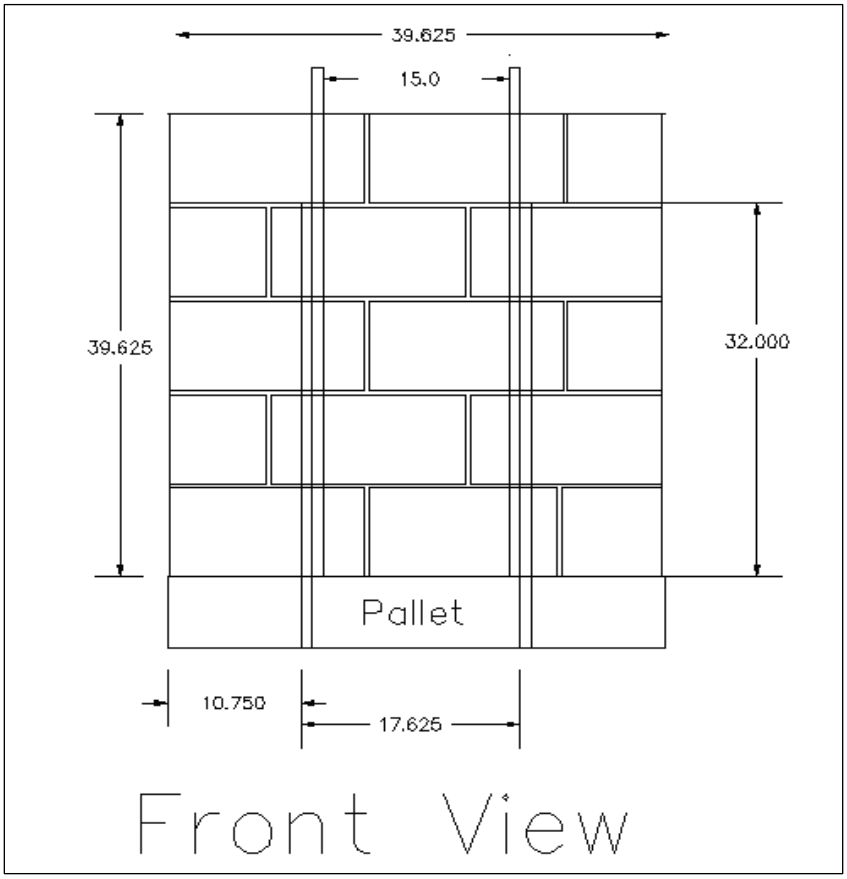

A fine-grout mix consisting of portland cement, masonry sand, and water was prepared. The fine-grout mix was configured as allowed by ASTM C476 (2018b) for masonry grout (approximately one part cement to three parts sand). Three of the four grout batches were reinforced with fibers. The grout mix (plain or with fiber reinforcement) was poured into the unit core holes that contained rebar, vibrated, and finished. Figure 12 shows the wallets prior to grouting. Figure 13 shows one of the fiber-reinforced grout mixes in the mixer. Figure 14 shows the cells receiving grout, and Figure 15 shows a fully grouted wallet specimen. After construction, all masonry wallets were cured in ambient laboratory conditions for a minimum of 28 days prior to testing.

Figure 12. Masonry wallets prior to grouting.

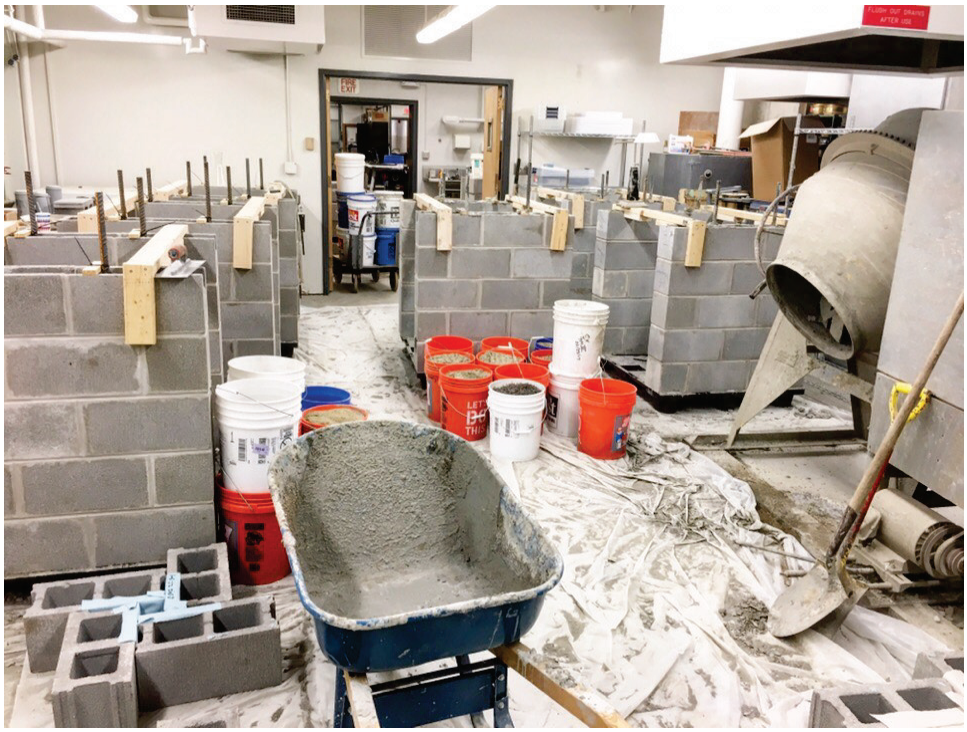

Figure 13. Fine grout and fiber in mixer.

Figure 14. Wallet specimens about to receive grout.

Figure 15. Wallet specimens after grouting.

For each grout batch, three rectangular (3.2-in. x 3.2-in. x 6.7-in.) grout compression test prisms were cast using the procedures in ASTM C476 (2018b; Figure 16). After a minimum curing of 28 days in the moist room, these prisms were capped with gypsum cement capping material and

tested for compressive strength using the procedures in ASTM C476 (2018b) over the period of masonry wallets testing (Figure 17).

Figure 16. Grout prism forms.

Figure 17. Grout prism capping.

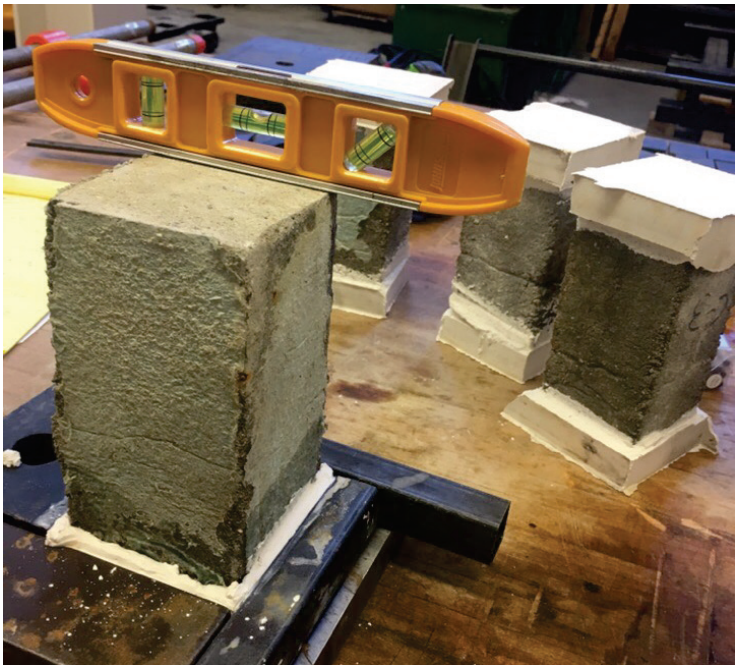

2.4 Masonry tests

After curing in the lab for a minimum of 28 days, each of the masonry wallets was placed in the loading frame shown in Figure 18. This loading frame was capable of withstanding up to a 100-k load and placed up to a 50-kip load on each of the embedded rebars. The lower part of the

loading frame consisted of four vertical 6-in. x 6-in. x 1/8-in. steel tubes. Two horizontal 6-in. x 4-in. x 3/8-in. tubes held the masonry wallet in place and prevented it from twisting during the test. The upper part of the frame was designed to provide greater stability of the entire system and to connect a 100-kip load cell and a 120-kip load cylinder to a 1.25-in.-diam, 100-kip capacity threaded bar. The rebars were connected to threaded bars by using a commercially available rebar coupler on both sides of the wallet. Four displacement sensors (one on each side of the exposed rebar) were attached to the wallet in order to measure rebar movement on each side of the specimen during testing.

Figure 18. Loading frame and masonry wallet specimen.

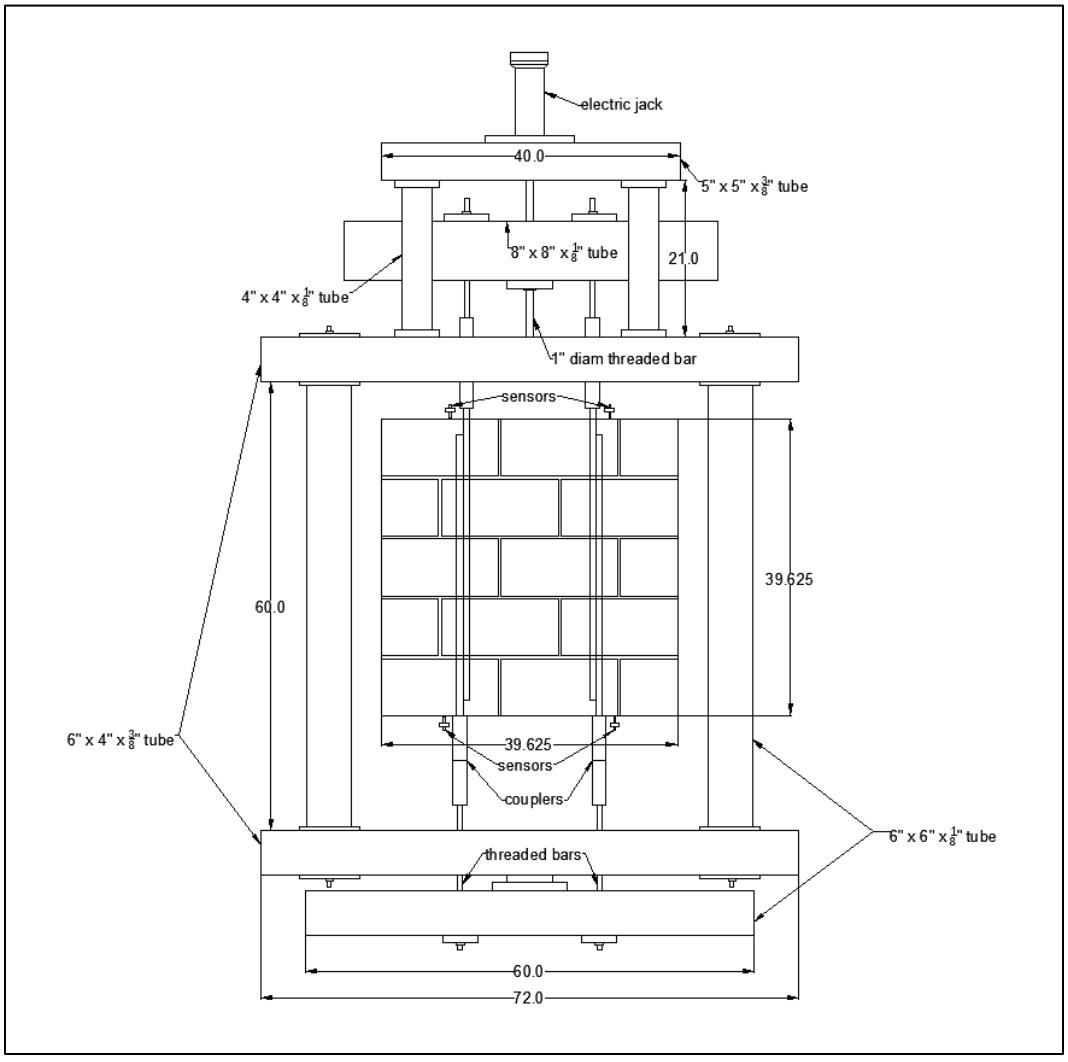

2.5 UHPC tests

UHPC is an emerging technology that has been used for critical components in concrete structures and a variety of other applications. The American Concrete Institute (ACI) defines UHPC as "concrete that has a minimum specified compressive strength of 150 MPa (22,000 psi) with specified durability, tensile ductility, and toughness requirements; fibers are generally included to achieve specified requirements" (2018).

The water-cement ratio of these materials is typically below 0.25 and even as low as 0.15. UHPC formulations typically contain large dosages of low-heat Portland cement or oil-well cement, siliceous or aluminous fine aggregates, crushed quartz or silica flour, silica fume, water, high-range water-reducing admixtures, and steel fibers. The addition of steel fibers is intended to offset brittle-like behavior that UHPCs exhibit as a result of their high compressive strengths. Steel fibers delocalize microcracks and localized cracks in UHPC, thereby increasing toughness and ductility.

The amount of steel fibers in UHPC formulations varies. For this study, UHPC formulations were produced with 1% steel fibers by volume. A 2% by volume dosage was attempted, but the steel fibers segregated from the UHPC material. Table 4 details the fiber configurations for the UHPC tests. The UHPC matrices were kept consistent across all four mixtures to ensure that a direct comparison between fibers could be made. The only variance was a slight difference in the high-range water-reducing admixture dosage, which was varied to achieve a similar rheology for each mixture. A consistent curing regime was implemented consisting of seven days at 72°F inside a fog room with 100% relative humidity and in accordance with ASTM C511 (2019a) followed by steam curing for seven days at 194°F. Following steam curing, the specimens were stored indoors at 73°F.

Table 4. UHPC test specimen configurations.

Test Method	Fiber Type
ASTM C1609 (2019b)	Coated steel fiber; Diam = 0.080 & 0.047 in., Length = 1.5 in.
	Uncoated steel fiber; Diam = 0.080 & 0.047 in., Length = 1.5 in.
ASTM C39 (2015)	Coated steel fiber; Diam = 0.080 & 0.047 in., Length = 1.5 in.
	Uncoated steel fiber; Diam = 0.080 & 0.047 in., Length = 1.5 in.
Nanoindentation	Coated steel fiber; Diam = 0.080 & 0.047 in., Length = 1.5 in.
	Uncoated steel fiber; Diam = 0.080 & 0.047 in., Length = 1.5 in.

2.5.1 Flexural tests

UHPC specimens were tested for flexural response according to ASTM C1609 (2019b). This test used 6-in. by 6-in. by 21-in. beams with four-point loading and an 18-in. span length. The span length was determined by multiplying the depth of the beam by three. Specimens were cast according to ASTM C192 (2018a) and consolidated on a vibrating table. Linear variable differential transformers (LVDTs) were used during flexural response testing to measure centerline deflection at 28 days. The ASTM 1609 (2019b) test setup is shown in Figure 19.

2.5.2 Compression tests

The unconfined compressive strength (UCS) of UHPC specimens was determined in accordance with ASTM C39 (2015). In accordance with ASTM C192 (2018a), 6-in. by 12-in. cylinders were cast in plastic molds. The larger cylinder size was used because of the length of the fibers. A vibrating table was used to consolidate the material in three approximately equal lifts. Cylinders were ground, when hardened, to ensure end planeness. A 1-million-lbf capacity universal testing machine was used to test the UHPC specimens after 28 days of curing.

Figure 19. ASTM 1609 (2019b) test setup.

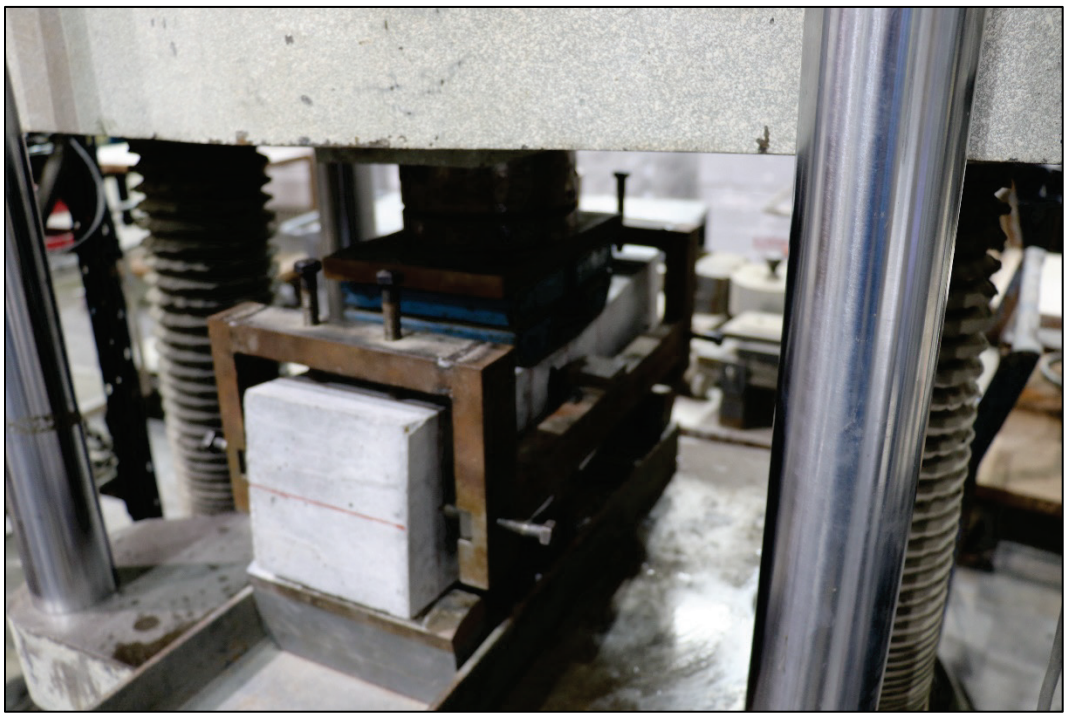

2.5.3 Nanoindentation tests

UHPC specimens were also tested for modulus across the interfacial transition zone (ITZ) of the UHPC matrix and the enamel coated fibers. An Agilent Technologies G200 nanoindenter was used to probe UHPC specimens. Test specimens were cast in 1-ft by 1-ft by 3-in. panels. Fibers were placed vertically into the fresh concrete. Once the concrete matrix hardened, the area around the vertical fibers was cored using a core bit with a 1.26-in. finish diameter. The core was then sawed into four equal sections by using a concrete saw. Of the four sections, two were used as nanoindentation specimens.

The specimens were submerged in a low-viscosity microscopy-grade epoxy in 1.25-in.-diam plastic molds. The epoxy was cured at ambient temperature for 24 hr. The samples were polished to 1,200 grit by using silicon carbide grinding pads with ethylene glycol as a polishing lubricant to minimize leaching of the mortar. Then, the samples were polished by using 9-µm, 3-µm, and 0.25-µm diamond paste applied to polishing pads with a low mineral solubility polishing lubricant. Examples of the test specimens are shown in Figure 20.

Figure 20. Nanoindentation test specimens.

The nanonindenter that probed the specimens used a pyramid-shaped diamond Berkovich indenter with an approximately 20-nm radius tip (Figure 21). A fused silica reference material was used to perform a second-order area function calibration prior to each measurement. The ITZ was probed in load control mode using a maximum load of 2 mN at a loading rate of 0.2 mN/s. The indenter placed 75 indents linearly in five regions of the ITZ in each sample with a 5-µm spacing between indents. The 6th indent of each region was in the enamel coating of the fiber.

Figure 21. Nanoindenter setup.

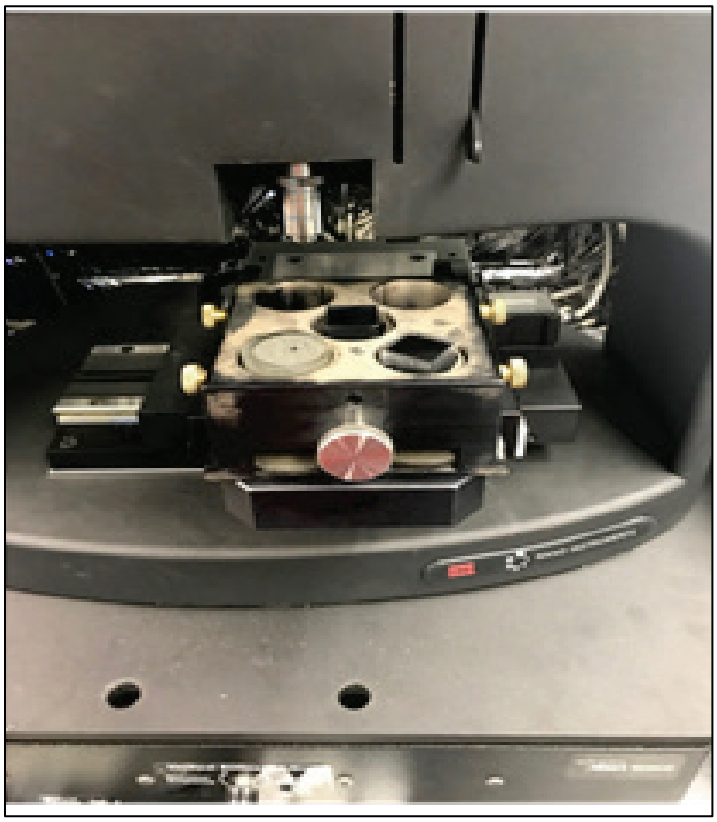

3 Tests Results

3.1 Concrete compression cylinder tests for the beams

The results of the concrete compression tests for the beam mixtures are shown in Table 5. None of these cylinders contained fibers. The material for each cylinder was extracted from the concrete mix prior to fiber additions for each batch, as noted in Table 5. These tests were conducted at an average age of 15 days. The average compressive strength of the plain concrete was 5,128 psi (within 2% of the design value of 5,000 psi). Also shown in the tables is the coefficient of variation for each sample set (CV).

Table 5. Concrete cylinder compression test results for beam concrete mix.

4x8 Control Cylinders (for beams with no fibers)						
Specimen No.	Date Made	Date Tested	Load (lb)	Compressive Strength	Mean Compression Strength	CV
S-1	03-26-2018	04-10-18	65,700	5,228	5,252	0.4%
S-2	03-26-2018	04-10-18	66,200	5,268		
S-3	03-26-2018	04-10-18	66,100	5,260		
4x8 Cylinders (for beams with 0.080-in.-diam fiber [coated/uncoated])						
Specimen No.	Date Made	Date Tested	Load (lb)	Compression Strength	Mean Compression Strength	CV
S-1	03-29-2018	04-13-2018	63,500	5,053	5,186	2.3%
S-2	03-29-2018	04-13-2018	65,700	5,228		
S-3	03-29-2018	04-13-2018	66,300	5,276		
4x8 Cylinders (for beams with 0.080-in.-diam or 0.047-in.-diam fiber blends [coated/uncoated])						
Specimen No.	Date Made	Date Tested	Load (lb)	Compression Strength	Mean Compression Strength	CV
S-1	03-30-2018	04-14-2018	63,500	5,053	4,947	2.0%
S-2	03-30-2018	04-14-2018	62,000	4,934		
S-3	03-30-2018	04-14-2018	61,000	4,854		

3.2 Beam test results

The three plain (control) concrete beam specimens -- S1, S2, and S3 -- deformed little under third-point loading until snapping through at peak cracking loads of 7,561 lb, 5,849 lb, and 6,234 lb, respectively. This produced an average peak load of 6,548 lb. The plain concrete beam

cracked in the central peak moment region, as shown in Figure 22. All beams were loaded initially with steel plates.

Figure 22. Plain concrete beams after cracking.

The load-deflection response of the beams reinforced with uncoated 0.080-in.-diam fiber (3% loading) is shown in Figure 23. All beams were loaded initially with steel plates underneath the beams. For these beams, deflection increased with load in a linear manner until near peak, where nonlinear deformation occurred. This nonlinear response was followed quickly with a load peak and a gradual falloff in load capacity with relatively large deflection. Near peak load, a large vertical crack was observed in the maximum moment region of the beam (Figure 24). Upon removal of the plate and reloading, the post-cracking responses of all three beams were similar, but there was a higher second peak load shown for Specimen 3 before a gradual falloff of load. Loading was stopped at about 0.15 in. due to travel limits on the sensors.

Figure 23. Load-deflection responses of uncoated 0.080-in.-diam fiber (3% loading) concrete beams.

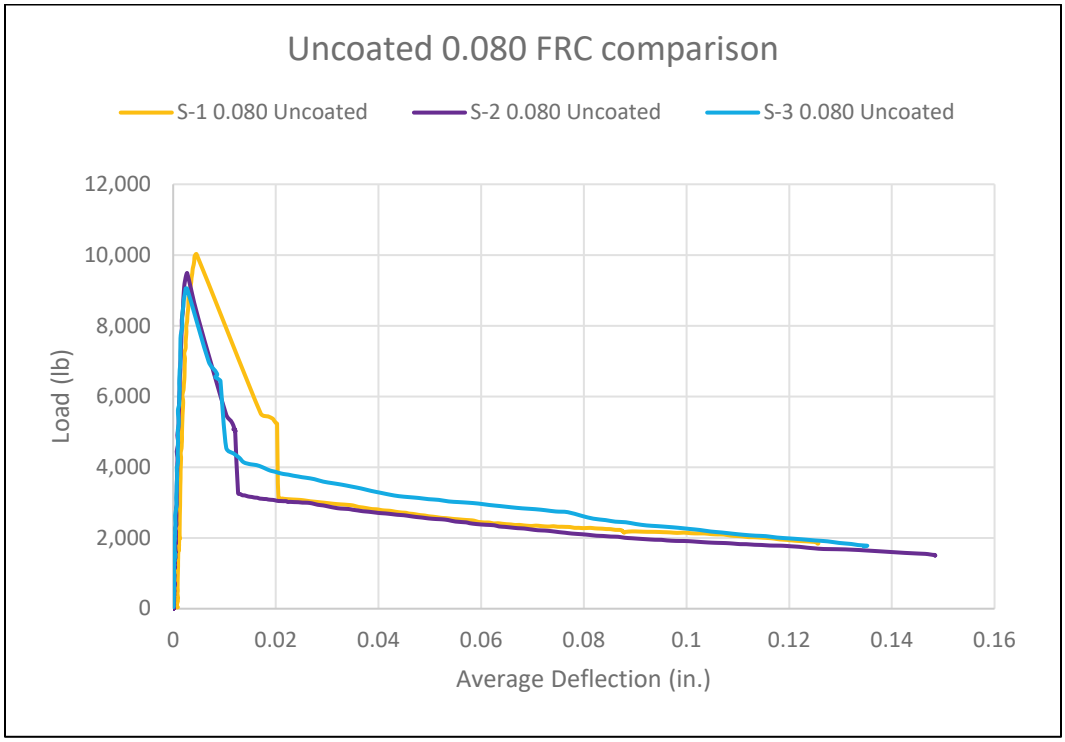

Figure 24. Uncoated 0.080-in.-diam fiber (3% loading) beam cracked configuration after peak loading.

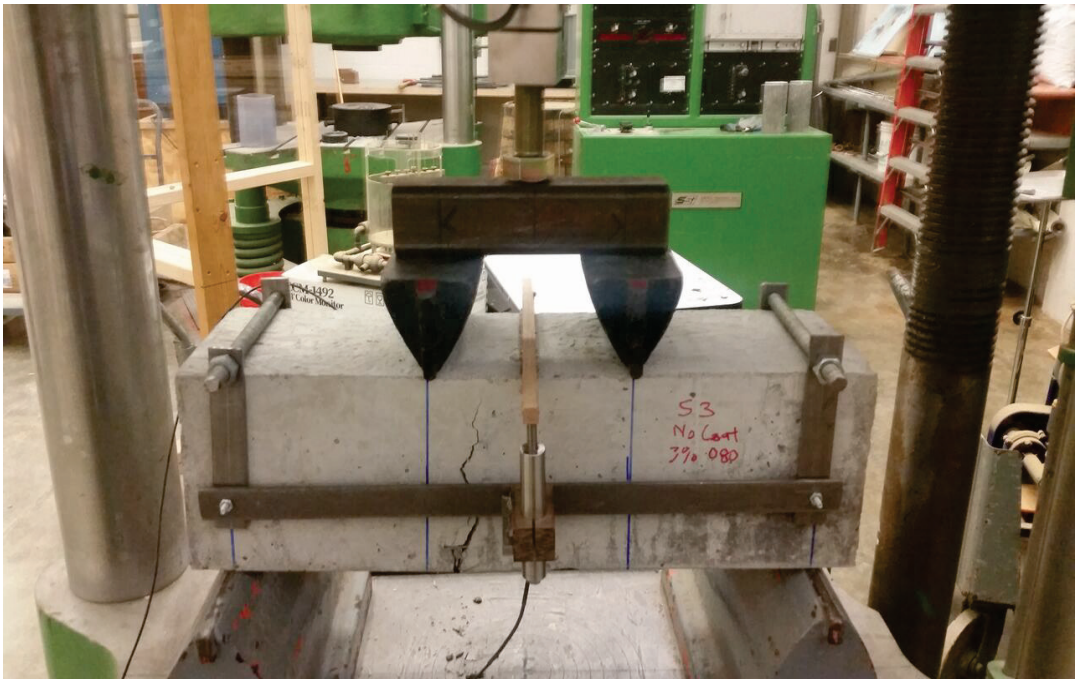

The load-deflection response of the beams reinforced with coated 0.080-in.-diam (3% loading) fibers is shown in Figure 25. All beams were loaded initially with steel plates. Deflections in these beams increased in a linear manner until near peak where nonlinear deformation occurred. This nonlinear response was followed quickly with a load peak. After load peak was reached, the plates were removed; and the beams were reloaded. Near load peak, vertical cracks were observed in the maximum moment region of the beam (Figure 26). Upon removal of the plate and reloading, the post-cracking responses of the three beams had more variability than in the case with uncoated 0.080 fibers. This could possibly happen due to a difficulty in fiber dispersion throughout the mix. Loading was stopped at about 0.15 in. due to travel limits on the sensors. Both cracking loads and post-cracking loads were much higher with the coated fiber, as compared to the uncoated fiber beams at the same fiber loading. Specimen 2 showed significantly higher load capacities than the other two specimens. This was likely due to random alignment of the fibers in the critical tension zone. There were qualitatively more fibers observed in this specimen in the critical area where cracking occurred.

Figure 25. Load-deflection response of coated 0.080-in.-diam fiber (3% loading) concrete beams.

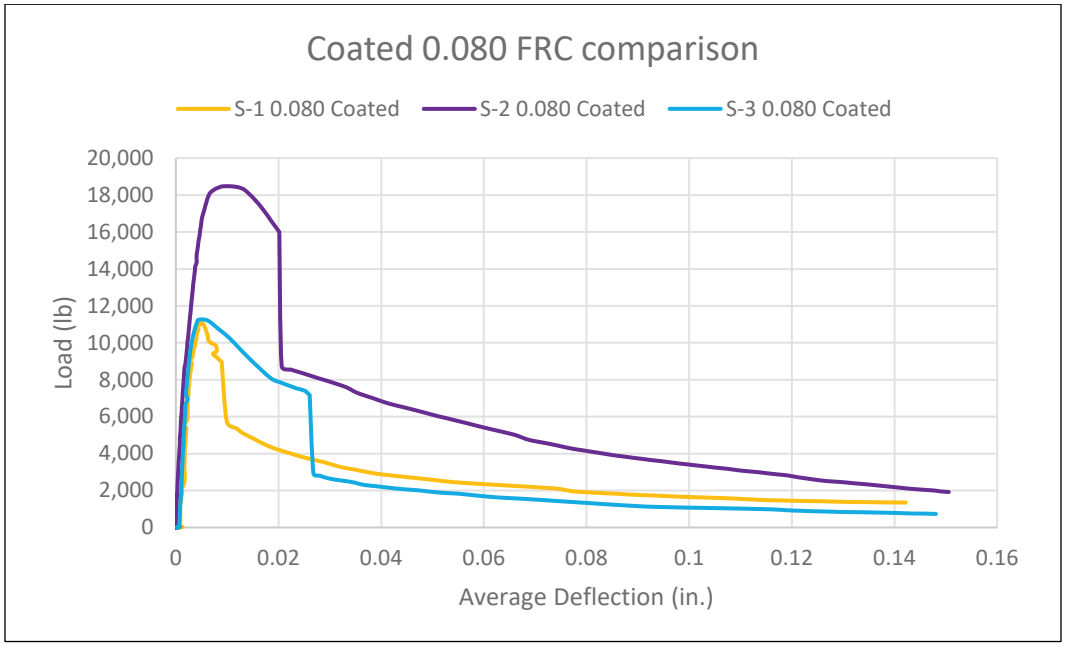

Figure 26. Coated 0.080-in.-diam fiber (3% loading) beam cracked configuration after peak loading.

The load-deflection response of the beams with an uncoated 0.080-in.-diam (1.5% loading) and 0.047-in.-diam (1.5% loading) fiber mix is shown in Figure 27. All three beams deflected in a linear manner until near peak where nonlinear deformation occurred. This nonlinear response was followed quickly with a load peak and a gradual falloff in load capacity with relatively large deflection. Near peak load, vertical cracks were observed in the maximum moment region of the beam (Figure 28). Specimen 2 showed higher results than Specimens 1 and 3; however, the overall responses among all three beams before and after removal of the plate were very similar. Loading was stopped near 0.1 in. due to travel limits on the sensors.

Figure 27. Load-deflection response of uncoated 0.080-in.-diam (1.5% loading) + 0.047-in.-diam fiber (1.5% loading) mix concrete beams.

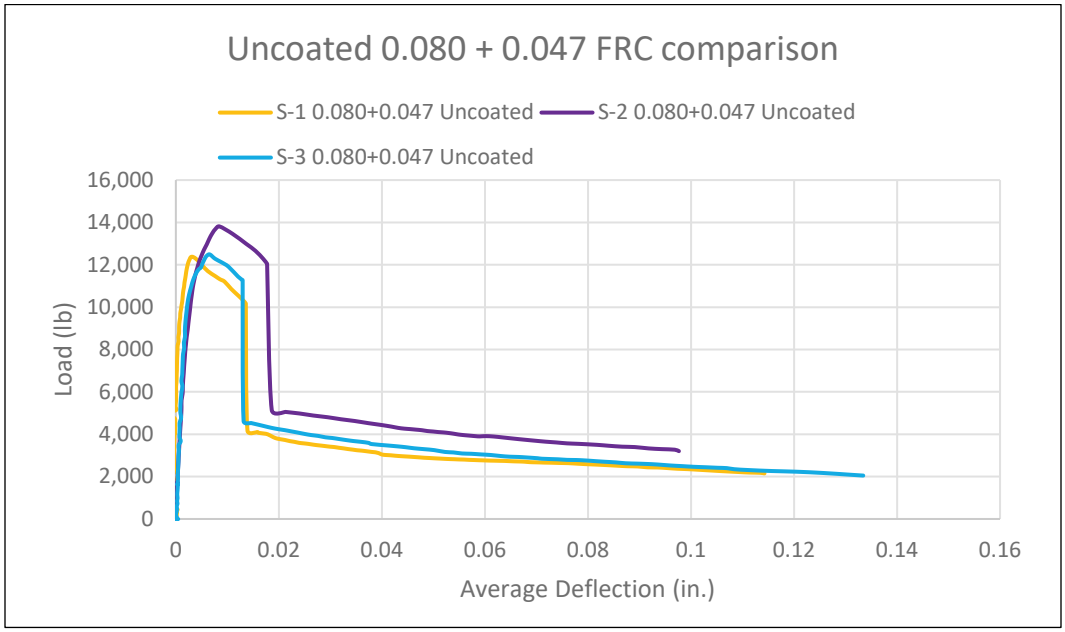

Figure 28. Uncoated 0.080-in.-diam fiber (1.5% loading) + 0.047-in.-diam fiber (1.5% loading) mix beam cracked configuration after peak loading.

The load-deflection responses of the beams with a coated 0.080-in.-diam (1.5% loading) and 0.047-in.-diam fiber (1.5% loading) mix are shown in

Figure 29. All three beams in this configuration deflected in a linear manner until near peak, where nonlinear deformation occurred. This nonlinear response was followed quickly with a load peak and a gradual falloff in load capacity with relatively large deflection. Near peak load, vertical cracks were observed in the maximum moment region of the beam (Figure 30). Upon removal of the plate and reloading, the post-cracking responses of all three beams were similar, but there was a much higher second peak shown for Specimen 1. This was most likely the result of variability of fiber orientation and loading in the area of maximum tensile stresses. Loading was stopped near 0.1 in. due to travel limits on the sensors. Both cracking loads and post-cracking loads were significantly higher for the coated 0.080+0.047 fiber mix-loading configuration compared to the uncoated one. Moreover, the coated 0.080+0.047 fiber mix showed the best results among all fiber configurations tested.

Figure 29. Load-deflection response of coated 0.080-in.-diam fiber (1.5% loading) + 0.047-in.-diam fiber (1.5% loading) mix concrete beams.

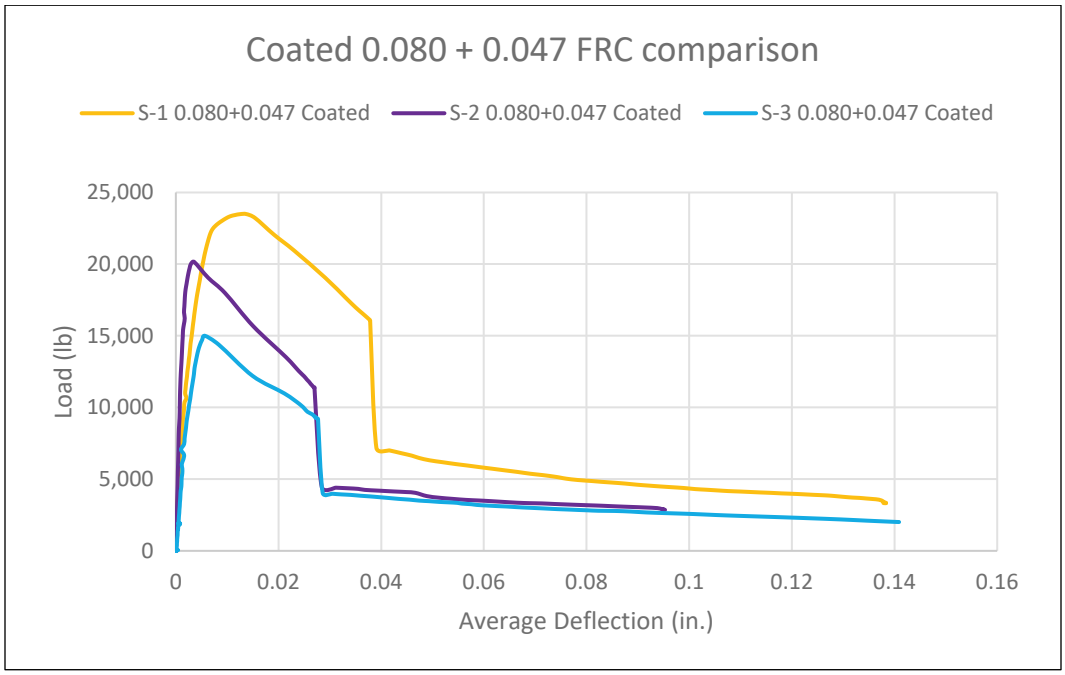

Figure 30. Coated 0.080-in.-diam + 0.047-in.-diam fiber mix beam cracked configuration after peak loading.

A summary of the beam test results for the four different fiber mix configurations as compared to the control is given in Table 6. The Modulus of Rupture (MOR) and the Average Residual Strength (ARS) were determined for each beam test using the procedures defined in ASTM C1399 (2016b) and are listed in Table 6. A comparison of the MORs of the fiber-reinforced beams to those of the plain concrete beams showed an increase in cracking strength of 1.5 times for uncoated 0.080 fibers to almost 3 times for the coated 0.080+0.047 mix.

Table 6. Concrete beam test results.

Specimen No.	Date Made	Date Tested	MOR (psi)	Average MOR (psi)	CV of MOR	ARS (psi)	Average ARS (psi)	CV of ARS
Control (Plain) Beams								
S-1	03-26-18	04-10-18	630	545	13.9%	-	-	-
S-2	03-26-18	04-10-18	485			-		
S-3	03-26-18	04-10-18	520			-		
0.080 Coated Beams								
S-1	03-29-18	04-13-18	925	1,135	30.8%	274	367	59.7%
S-2	03-29-18	04-13-18	1,540			618		
S-3	03-29-18	04-13-18	945			210		
0.080 Uncoated Beams								
S-1	03-29-18	04-12-18	835	855	9.3%	240	254	11.7%
S-2	03-29-18	04-12-18	790			234		
S-3	03-29-18	04-13-18	945			288		
0.080 + 0.047 Coated Beams								
S-1	03-30-18	04-13-18	1,960	1,630	21.9%	612	430	36.8%
S-2	03-30-18	04-13-18	1,680			354		
S-3	03-30-18	04-13-18	1,250			324		
0.080 + 0.047 Uncoated Beams								
S-1	03-30-18	04-13-18	1,030	1,075	6.2%	274	313	13.5%
S-2	03-30-18	04-13-18	1,150			358		
S-3	03-30-18	04-13-18	1,040			308		

Table 6 data also show that, in general, coated fiber mixes have much higher MORs and ARSs, although the uncoated fiber mixes showed lower variation.

When comparing the performances of the two different fiber diameters, the concrete mixes of 0.080- and 0.047-in.-diam fibers showed much higher strengths than that of the 0.080-in.-diam mix. This appears to indicate that thinner fibers work better (produce greater increases in strength and ductility) in the concrete mix. A possible reason for this is the fact that for the same concrete mix, better flow is achieved when smaller

diameter fibers are used. It therefore is easier for fibers to disperse throughout the mix, resulting in a much better performance.

3.3 Compression test results

3.3.1 Set No. 1 – control

The control (no fibers) cylinders demonstrated typical behavior for unreinforced concrete under compression. Figure 31 shows the cylinders after stripping of the forms. There were no significant voids. The cylinder prior to testing with the extensometer attached is shown in Figure 32. The evenly distributed vertical cracks the cylinders experienced right after failure are shown in Figure 33. The compression stress-strain response of the control cylinders is shown in Figure 34. There is little ductility in post-cracking behavior.

Figure 31. Control compression test cylinders before testing.

Figure 32. Control compression test cylinders ready for testing.

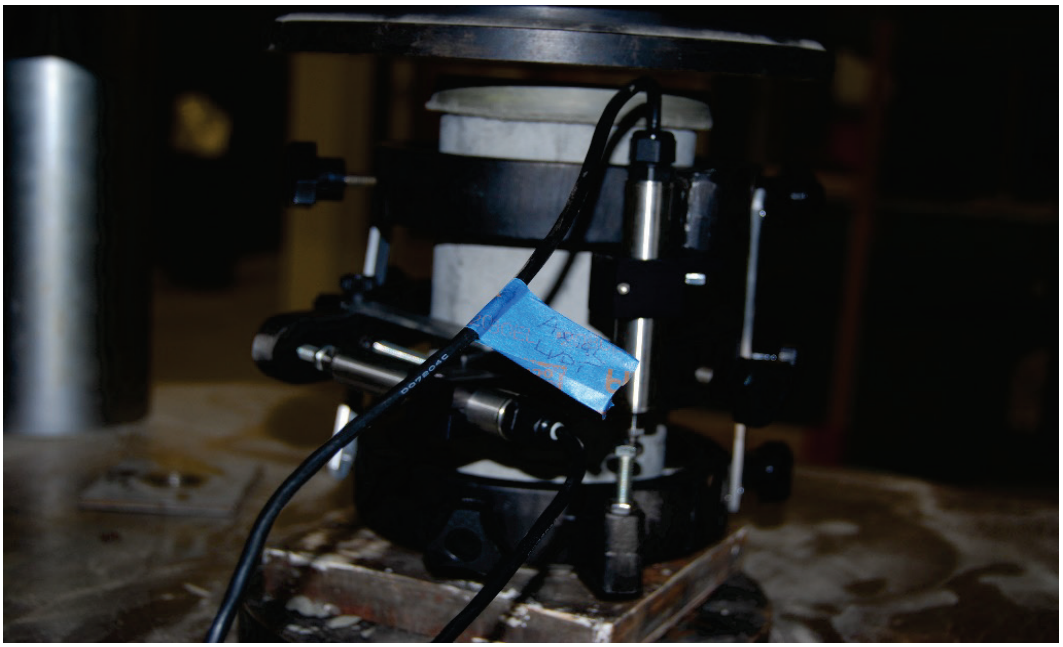

Figure 33. Control compression test cylinders after testing.

Figure 34. Compression stress-strain response of control cylinders.

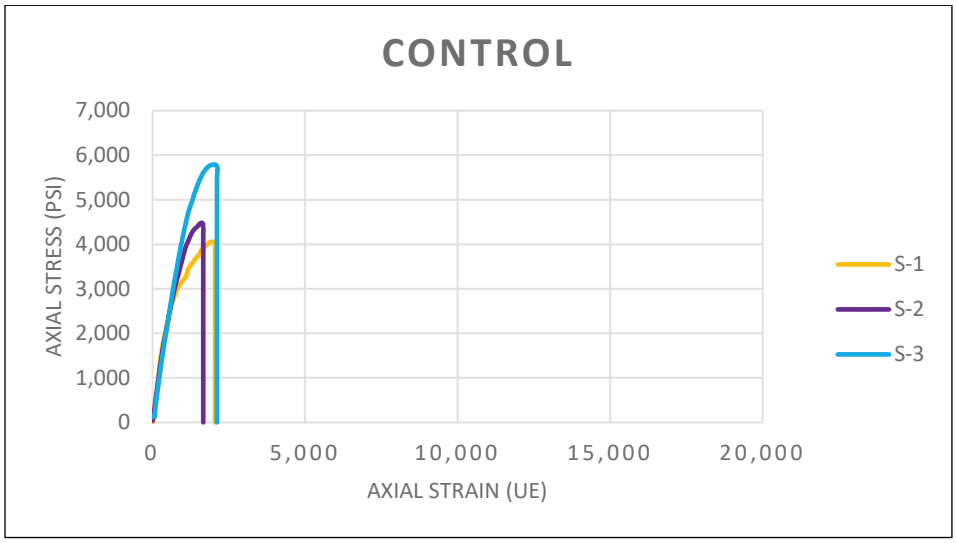

A summary of the compression test results for the nine different fiber mix configurations is shown in Table 7. Also shown are the average and CVs for each of the test sets.

In addition, the area under the stress-strain response for each of the tests was determined by using numerical integration. This is the modulus of toughness and was determined as a measure of the ductility of the material. The average and CV for each of the configurations are also shown in Table 7.

Table 7. Result of the compression tests for fiber concrete cylinders.

4x8 Control Cylinders (no fibers)								
Specimen No.	Date Made	Date Tested	Compressive Strength (psi)	Mean Compressive Strength (psi)	CV	Ductility (Modulus of Toughness, psi)	Average Ductility (psi)	CV
S-1	06-15-18	06-30-18	4,058	4,777	18.9%	5.94E+06	6.05E+06	23%
S-2	06-15-18	06-30-18	4,482			4.69E+06		
S-3	06-15-18	06-30-18	5,791			7.51E+06		
4x8 Cylinders Made with Coated 0.047 Fibers (1% loading)								
Specimen No.	Date Made	Date Tested	Compressive Strength (psi)	Mean Compressive Strength (psi)	CV	Ductility (Modulus of Toughness, psi)	Average Ductility (psi)	CV
S-1	06-15-18	07-02-18	5,529	5,968	7.4%	3.66E+07	3.15E+07	34%
S-2	06-15-18	07-02-18	5,960			3.87E+07		
S-3	06-15-18	07-02-18	6,416			1.93E+07		

4x8 Cylinders Made with Coated 0.047 Fibers (3% loading)								
Specimen No.	Date Made	Date Tested	Compressive Strength (psi)	Mean Compressive Strength (psi)	CV	Ductility (Modulus of Toughness, psi)	Average Ductility (psi)	CV
S-1	06-15-18	07-02-18	6,196	5,540	11.0%	6.35E+07	6.22E+07	16%
S-2	06-15-18	07-02-18	5,439			5.16E+07		
S-3	06-15-18	07-02-18	4,987			7.15E+07		
4x8 Cylinders Made with Coated 0.029 Fibers (1% loading)								
Specimen No.	Date Made	Date Tested	Compressive Strength (psi)	Mean Compressive Strength (psi)	CV	Ductility (Modulus of Toughness, psi)	Average Ductility (psi)	CV
S-1	06-15-18	06-30-18	2,637	2,749	5.7%	4.45E+07	4.08E+07	19%
S-2	06-15-18	06-30-18	2,682			4.61E+07		
S-3	06-15-18	06-30-18	2,929			3.19E+07		
4x8 Cylinders Made with Coated 0.029 Fibers (3% loading)								
Specimen No.	Date Made	Date Tested	Compressive Strength (psi)	Mean Compressive Strength (psi)	CV	Ductility (Modulus of Toughness, psi)	Average Ductility (psi)	CV
S-1	06-15-18	06-30-18	4,780	4,270	21.3%	8.63E+07	7.01E+07	33%
S-2	06-15-18	06-30-18	4,808			8.02E+07		
S-3	06-15-18	06-30-18	3,222			4.38E+07		
4x8 Cylinders Made with Uncoated 0.029 Fibers (1% loading)								
Specimen No.	Date Made	Date Tested	Compressive Strength (psi)	Mean Compressive Strength (psi)	CV	Ductility (Modulus of Toughness, psi)	Average Ductility (psi)	CV
S-1	06-19-18	06-30-18	4,589	4,579	2.3%	2.22E+07	**3.64E+07**	**62%**
S-2	06-19-18	06-30-18	4,470			2.44E+07		
S-3	06-19-18	06-30-18	4,678			6.24E+07		
4x8 Cylinders Made with Uncoated 0.029 Fibers (3% loading)								
Specimen No.	Date Made	Date Tested	Compressive Strength (psi)	Mean Compressive Strength (psi)	CV	Ductility (Modulus of Toughness, psi)	Average Ductility (psi)	CV
S-1	06-19-18	06-30-18	3,410	2,039	58.3%	5.67E+07	3.36E+07	60%
S-2	06-19-18	06-30-18	1,301			2.13E+07		
S-3	06-19-18	06-30-18	1,406			2.27E+07		
4x8 Cylinders Made with Coated 0.080 Fibers (3% loading)								
Specimen No.	Date Made	Date Tested	Compressive Strength (psi)	Mean Compressive Strength (psi)	CV	Ductility (Modulus of Toughness, psi)	Average Ductility (psi)	CV
S-1	06-19-18	07-02-18	3,313	4,406	28.8%	2.69E+07	3.54E+07	55%
S-2	06-19-18	07-02-18	5,800			5.78E+07		
S-3	06-19-18	07-02-18	4,104			2.16E+07		

4x8 Cylinders Made with Uncoated 0.080 Fibers (3% loading)								
Specimen No.	Date Made	Date Tested	Compressive Strength (psi)	Mean Compressive Strength (psi)	CV	Ductility (Modulus of Toughness, psi)	Average Ductility (psi)	CV
S-1	06-19-18	07-02-18	4,326	4,212	21.2%	5.31E+07	4.39E+07	23%
S-2	06-19-18	07-02-18	5,045			4.57E+07		
S-3	06-19-18	07-02-18	3,266			3.30E+07		
4x8 Cylinders Made with 0.047 Uncoated Fibers (1% loading)								
Specimen No.	Date Made	Date Tested	Compressive Strength (psi)	Mean Compressive Strength (psi)	CV	Ductility (Modulus of Toughness, psi)	Average Ductility (psi)	CV
S-1	06-19-18	07-02-18	4,151	4,308	5.9%	3.28E+07	3.35E+07	19%
S-2	06-19-18	07-02-18	4,590			2.74E+07		
S-3	06-19-18	07-02-18	4,182			4.04E+07		

3.3.2 Set No. 2 – 0.047-in.-diam coated fibers (1% loading)

The compression cylinders with coated 0.047-in.-diam fibers (1% loading) before and after compression tests are shown in Figures 35 and 36, respectively. The compression stress-strain response for this fiber-reinforced concrete is shown in Figure 37. During loading, strain of the concrete initially increased with load in a linear manner, showing elastic behavior, which was then followed by a non-elastic curve until it reached its peak stress. All three cylinders had a similar pre-crack behavior, with an average compressive strength of 5,968 psi and CV of 7.4% (Table 7).

Figure 35. Cylinders made with coated 0.047-in.-diam fiber (1% loading) before testing.

Figure 36. Cylinders made with coated 0.047-in.-diam fiber (1% loading) after testing.

Figure 37. Compression stress-strain response of cylinder with coated 0.047-in.-diam coated fiber (1% loading).

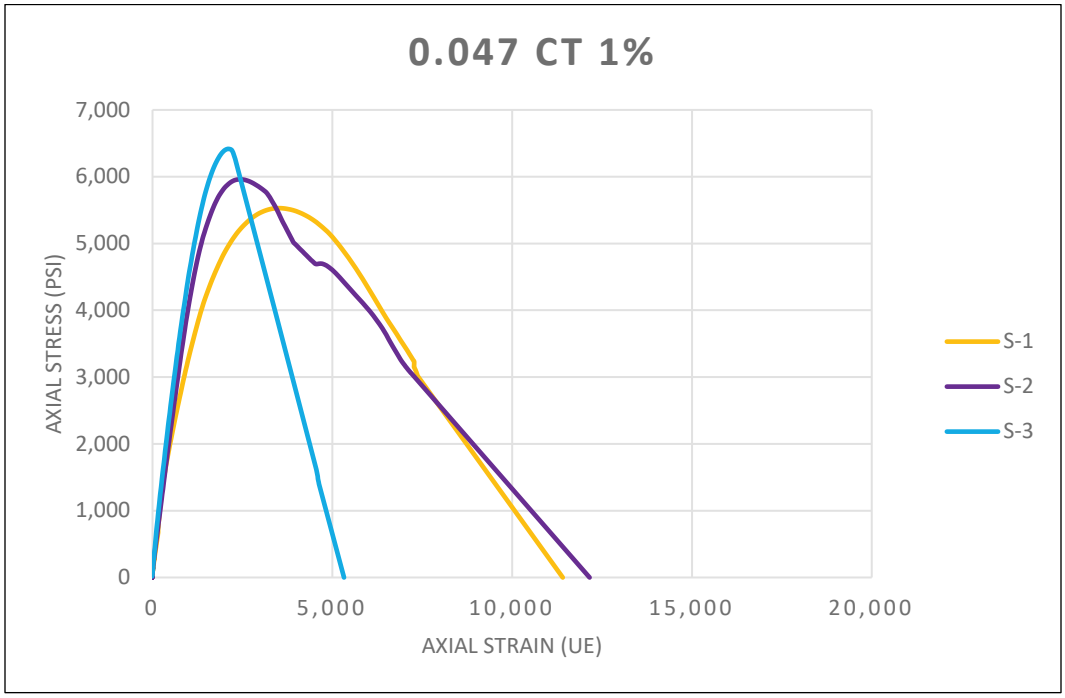

3.3.3 Set No. 3 – 0.047-in.-diam coated fibers (3% loading)

Cylinders of concrete formed with coated 0.047-in.-diam fibers (3% loading) before and after the compression tests are shown in Figures 38 and 39, respectively. The compression stress-strain responses for this fiber-reinforced concrete are shown in Figure 40. During loading, strain of the concrete initially increased with load in a linear manner showing elastic behavior, which was then followed by a non-elastic curve until it reached its peak stress. All three cylinders exhibited similar pre-crack behavior, with an average compressive strength of 5,540 psi and a CV of 11.0%.

All the cylinders after testing had vertical cracks evenly distributed over their surfaces. Figure 40 shows the compression stress-strain behavior of these cylinders. Specimen 3 shows the lowest peak load and the most ductile post-peak behavior. This may have occurred because the cap on the cylinder was not perfectly straight, causing an uneven loading and, thus, non-uniform stresses. All the cylinders from this set had a relatively gradual falloff in load capacity and reached a large strain value relative to the control set.

Figure 38. Cylinders made with coated 0.047-in.-diam fiber (3% loading) before test.

Figure 39. Cylinders made with coated 0.047-in.-diam fiber (3% loading) after test.

Figure 40. Compression stress-strain behavior of cylinders with coated 0.047-in.-diam fiber (3% loading).

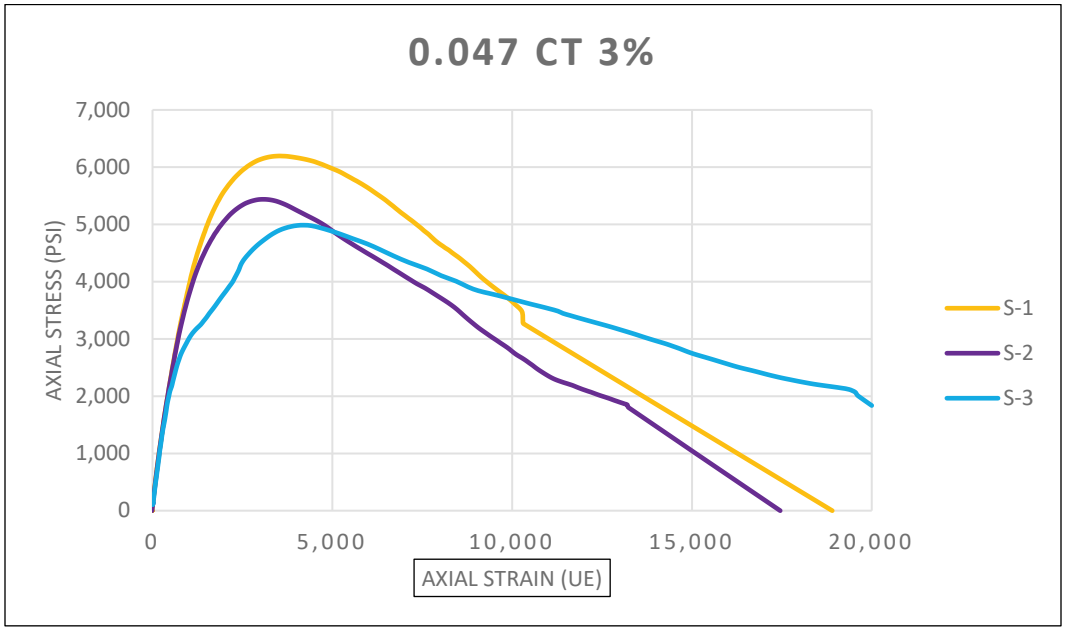

3.3.4 Set No. 4 – 0.029-in.-diam coated fibers (1% loading)

Cylinders made with coated 0.029-in.-diam fibers (1% loading) before and after compression tests are shown in Figures 41 and 42, respectively. Figure 43 shows the compression stress-strain response of each of the cylinders. During initial loading, strain of the concrete increased in a linear manner, followed by a nonlinear curve until it reached its peak. All three cylinders had a similar pre- and post-peak behavior. A significant reduction in compressive strength relative to the control set was shown, with an average value of 2,749 psi and a CV of 5.7%.

After testing, all the cylinders had vertical cracks evenly distributed over their surfaces. All of the specimens showed very high ductility. However, specimen 1 reached the highest strain value of all cylinders tested. This may have been caused by a cap on the cylinder that was not perfectly straight, producing an uneven loading and lower results. In general, all the cylinders from this set had a gradual falloff in load capacity and reached a relatively large strain value.

Figure 41. Cylinders made with coated 0.029-in.-diam fiber (1% loading) before testing.

Figure 42. Cylinders made with coated 0.029-in.-diam fiber (1% loading) after testing.

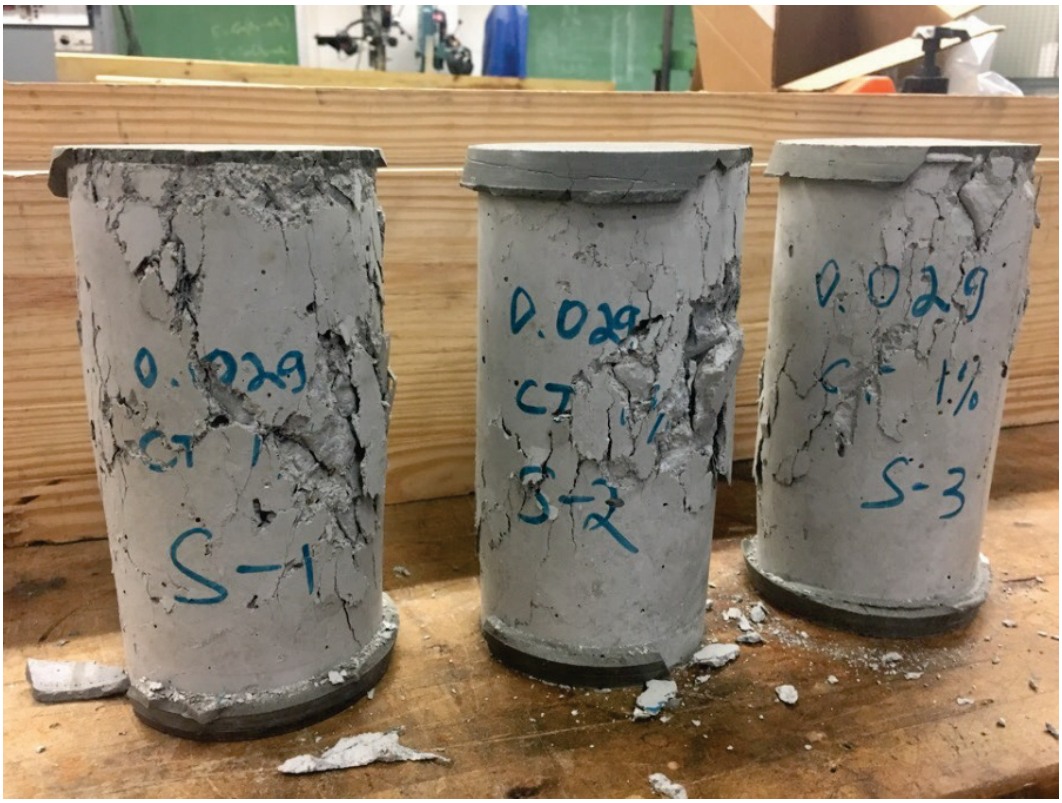

Figure 43. Compression stress-strain behavior of cylinders with coated 0.029-in.-diam fiber (1% loading).

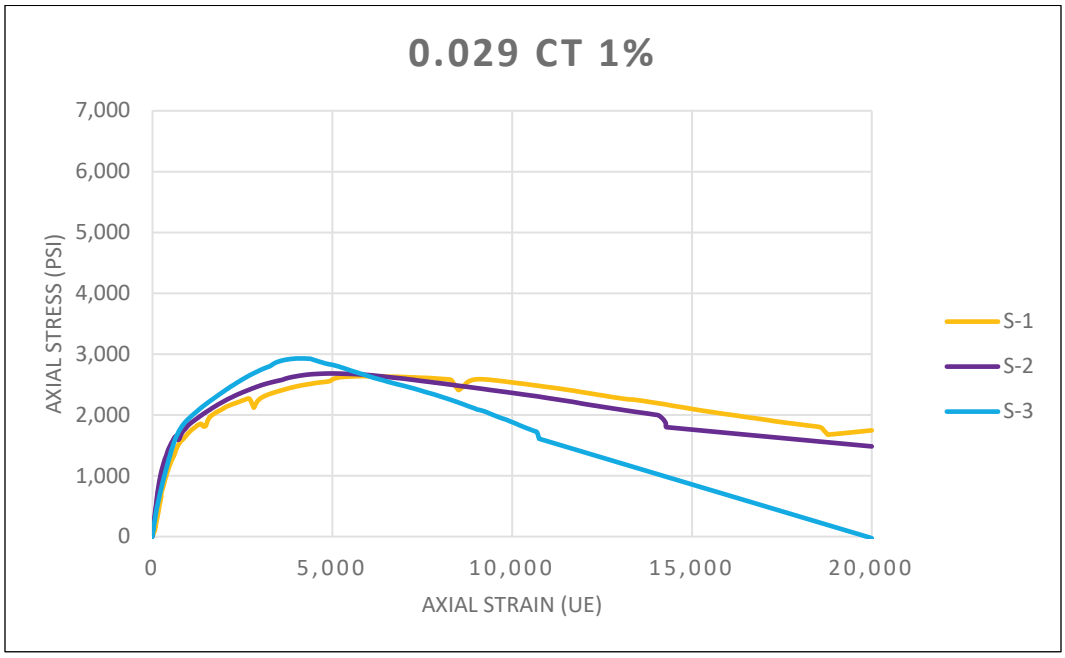

3.3.5 Set No. 5 – 0.029-in.-diam coated fibers (3% loading)

Cylinders with coated 0.029-in.-diam fibers (3% loading) before and after compression testing are shown in Figures 44 and 45, respectively. The compression stress-strain responses of the specimens are shown in Figure 46. During initial loading, the strain of the concrete increased with load in a linear manner, followed by a nonlinear response until the peak load was reached. All three cylinders demonstrated a similar pre-crack behavior. However, one of the three specimens had a consolidation problem (voids) that caused a significantly lower compressive strength than the other two (3,222 psi vs. 4,780 psi and 4,808 psi). Thus, the average strength was 4,270 psi, and a large CV of 21.3% was observed.

The tested cylinders exhibited several vertical cracks evenly distributed over their surfaces. All specimens showed a relatively high ductility in their post-peak behavior (Figure 46). However, Specimens 1 and 2 had higher final stresses than Specimen 3 likely due to poor consolidation typical of the higher fiber loading concrete configurations. In general, all the cylinders from this set had a gradual falloff in load capacity and reached a large final strain value.

Figure 44. Cylinders made with coated 0.029-in.-diam fiber (3% loading) before testing.

Figure 45. Cylinders made with coated 0.029-in.-diam fiber (3% loading) after testing.

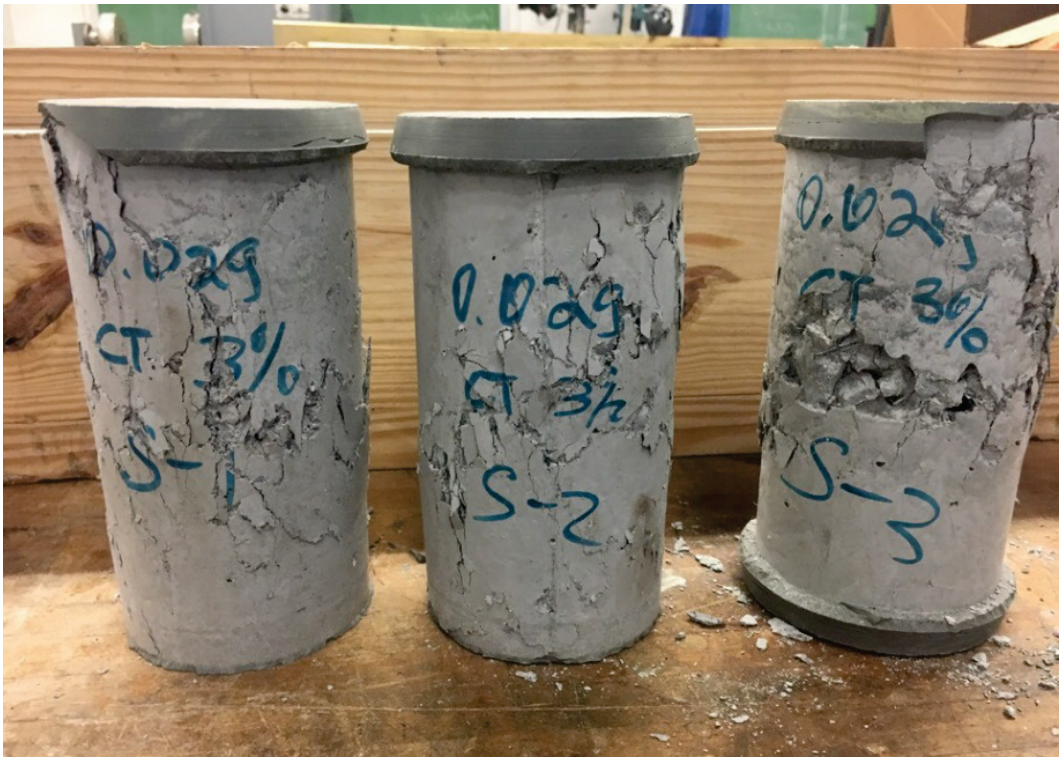

Figure 46. Compression stress-strain behavior of cylinders with coated 0.029-in.-diam fiber (3% loading).

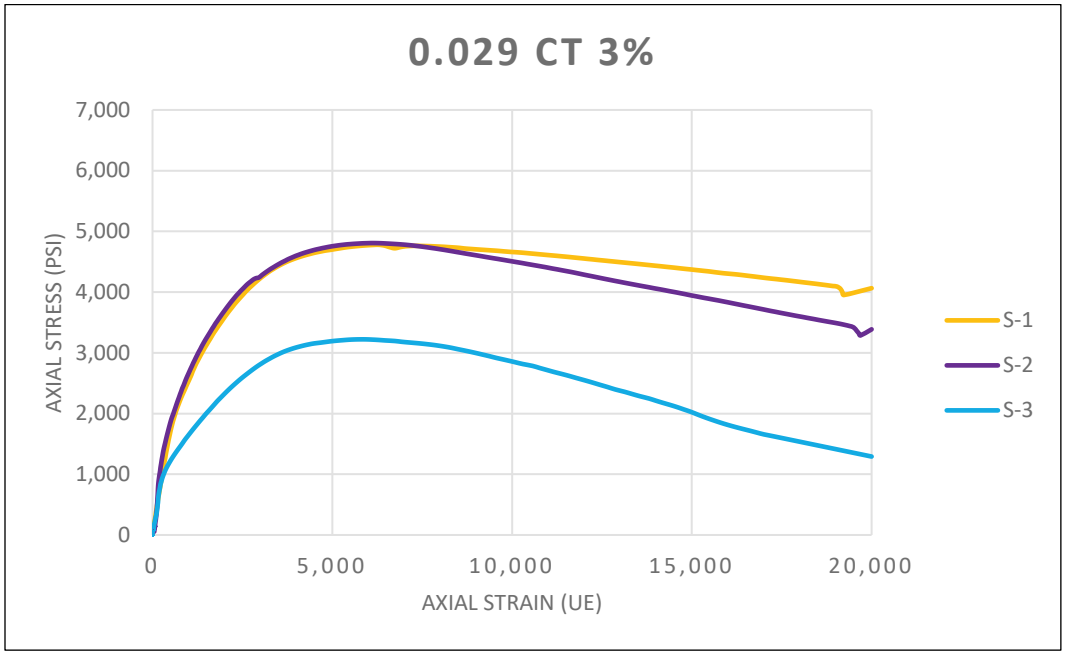

3.3.6 Set No. 6 – 0.029-in.-diam uncoated fibers (1% loading)

Cylinders with uncoated 0.029-in.-diam fibers (1% loading) before and after compression tests are shown in Figures 47 and 48, respectively. The compression stress-strain responses of the specimens are shown in Figure 49. During initial loading, the strain of the concrete increased with load in a linear manner, followed by a non-elastic response until the peak load was reached. All three cylinders had very similar pre-crack behavior with an average compressive strength of 4,579 psi and a CV of 2.3%.

All three cylinders had vertical cracks on their surfaces. However, Specimen 3 seemed to crack much more than Specimens 1 and 2. Specimen 3 also was the only one of three specimens showing a gradual fall-off in load capacity with deformation. The other two specimens exhibited a more brittle and sudden failure (Figure 49).

Figure 47. Cylinders made with uncoated 0.029-in.-diam fiber (1% loading) before testing.

Figure 48. Cylinders made with uncoated 0.029-in.-diam fiber (1% loading) after testing.

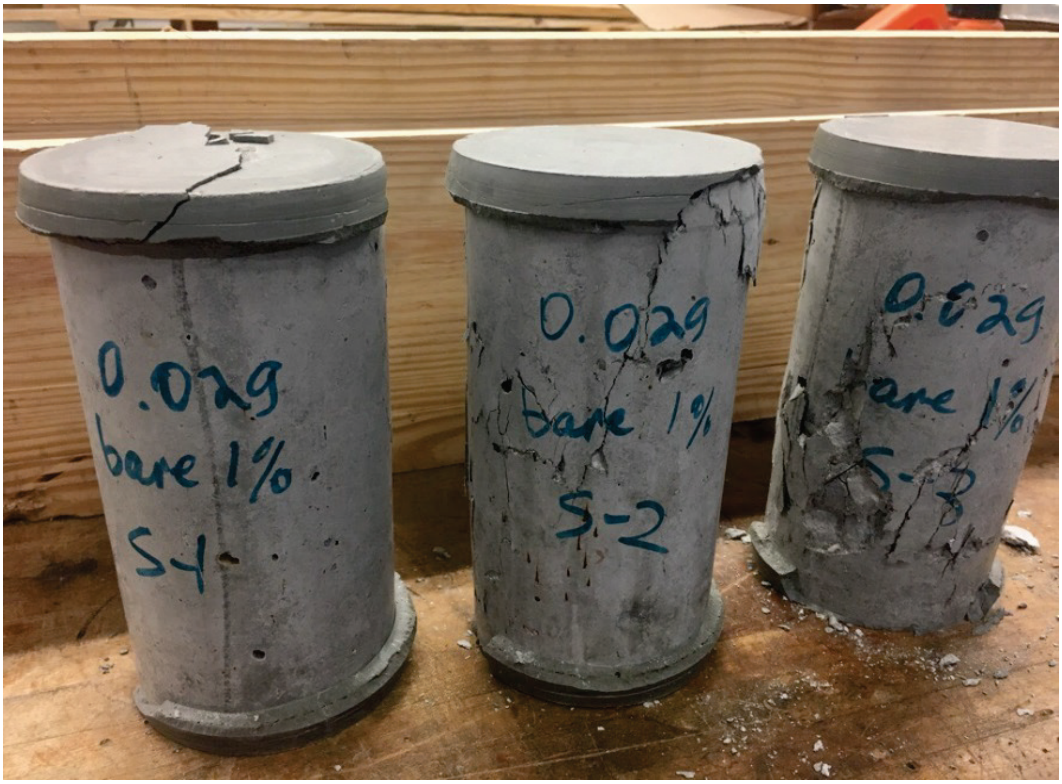

Figure 49. Compression stress-strain behavior of cylinders with uncoated 0.029-in.-diam fiber (1% loading).

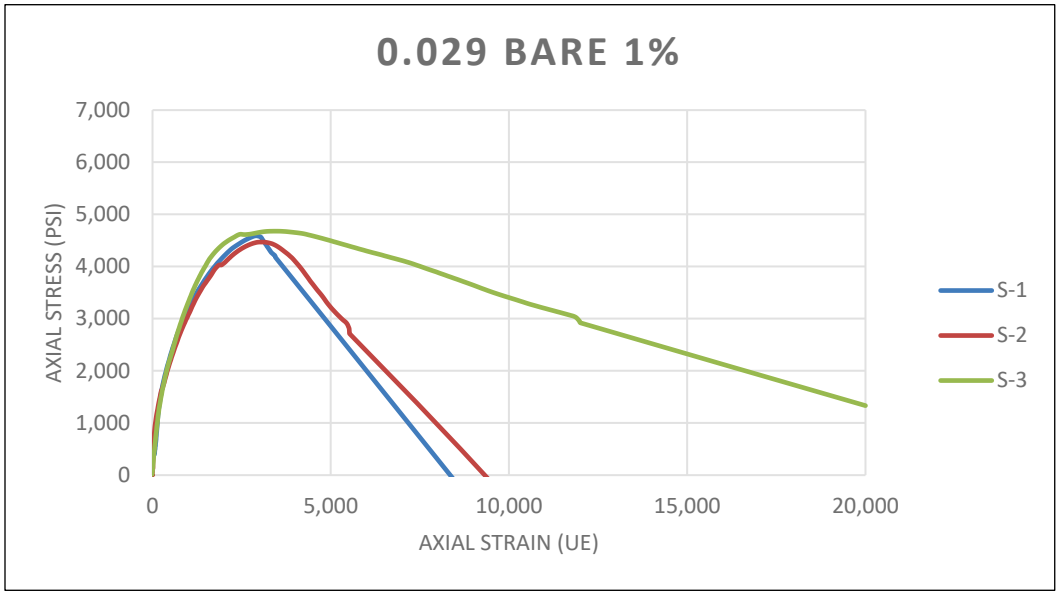

3.3.7 Set No. 7 – 0.029-in.-diam uncoated fibers (3% loading)

Compression specimens with uncoated 0.029-in.-diam fibers (3% loading) before and after compression tests are shown in Figures 50 and 51, respectively. Figure 52 shows the compression stress-strain responses of the specimens. During initial loading, the strain of the concrete increased with load in a linear manner, followed by a nonlinear response until the peak load was reached.

All three cylinders demonstrated a similar pre-crack behavior with a significant reduction in compressive strength relative to the control set. Only one of three specimens reached a compressive strength of 3,410 psi, while the other two showed strengths in the 1,300-psi range, resulting in a mean value of 2,039 psi and a very large CV of 58.3%.

Two of the three cylinders had poor consolidation (a problem with all the large fiber volume configurations) with many voids. This mix was particularly challenging to finish because of the nature of uncoated thin fibers. When a large volume of fibers is added to the mix, it is very hard to distribute them evenly, which made the mix difficult to finish and consolidate.

Figure 50. Cylinders made with uncoated 0.029-in.-diam fiber (3% loading) before testing.

Figure 51. Cylinders made with uncoated 0.029-in.-diam fiber (3% loading) after testing.

Figure 52. Compression stress-strain behavior of cylinders with uncoated 0.029-in.-diam fiber (3% loading).

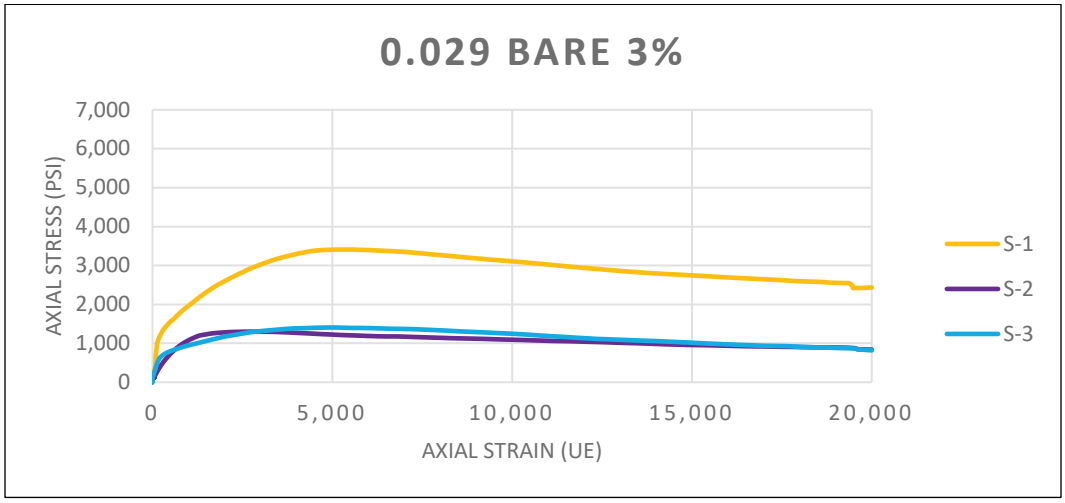

3.3.8 Set No. 8 – 0.080-in.-diam coated fibers (3% loading)

Cylinders with coated 0.080-in.-diam (3% loading) fibers before and after compression tests are shown in Figures 53 and 54, respectively. The compression stress-strain responses of the specimens are shown in Figure 55. During initial loading, the strain of the concrete increased

with load in a linear manner followed by a non-elastic response until the peak load was reached.

Figure 53. Cylinders made with coated 0.080-in.-diam fiber (3% loading) before testing.

Figure 54. Cylinders made with coated 0.080-in.-diam fiber (3% loading) after testing.

All three cylinders showed similar pre-crack behavior, but with a large variability in compressive strength values. Specimen 1 has the lowest strength, because the cylinder had consolidation issues, with a portion of its area showing exposed aggregate with concrete missing on the sides. The average compressive strength value for this set was 4,406 psi with a CV of 28.8%.

The post-peak behavior of the cylinders was relatively ductile, except for the specimen with bad consolidation (Figure 55).

Figure 55. Compression stress-strain behavior of cylinders with coated 0.080-in.-diam fiber (3% loading).

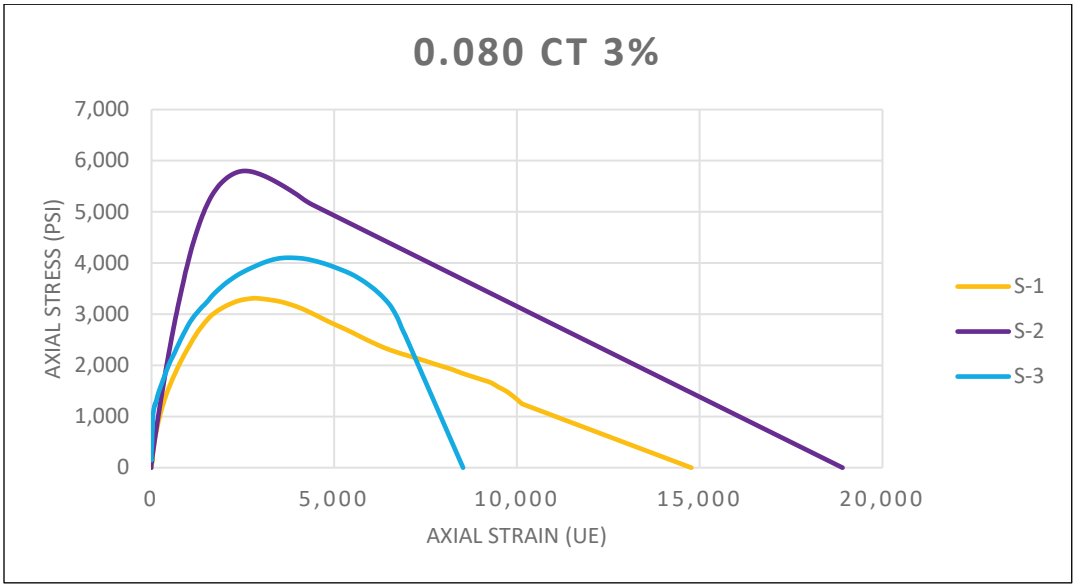

3.3.9 Set No. 9 – 0.080-in.-diam uncoated fibers (3% loading)

Cylinders with uncoated 0.080-in.-diam fibers (3% loading) after compression tests are shown in Figure 56. The compression stress strain response of the specimens is shown in Figure 57. During initial loading, the strain of the concrete increased with load in a linear manner, followed by a nonlinear response until the peak load was reached.

Figure 56. Cylinders made with uncoated 0.080-in.-diam fiber (3% loading) after testing.

All three cylinders show relatively similar pre-crack behavior but with a large variability of compressive strength values. Specimen 3 has the lowest strength because the cylinder had consolidation issues, with a portion of its area showing exposed aggregate with concrete missing on the sides. The average compressive strength value for this set was 4,212 psi with a CV of 21.0%.

The post-peak behavior of the cylinders was relatively ductile, with Specimen 1 reaching the highest strain of all cylinders tested (Figure 57).

Figure 57. Compression stress-strain behavior of cylinders made with uncoated 0.080-in.-diam (3% loading).

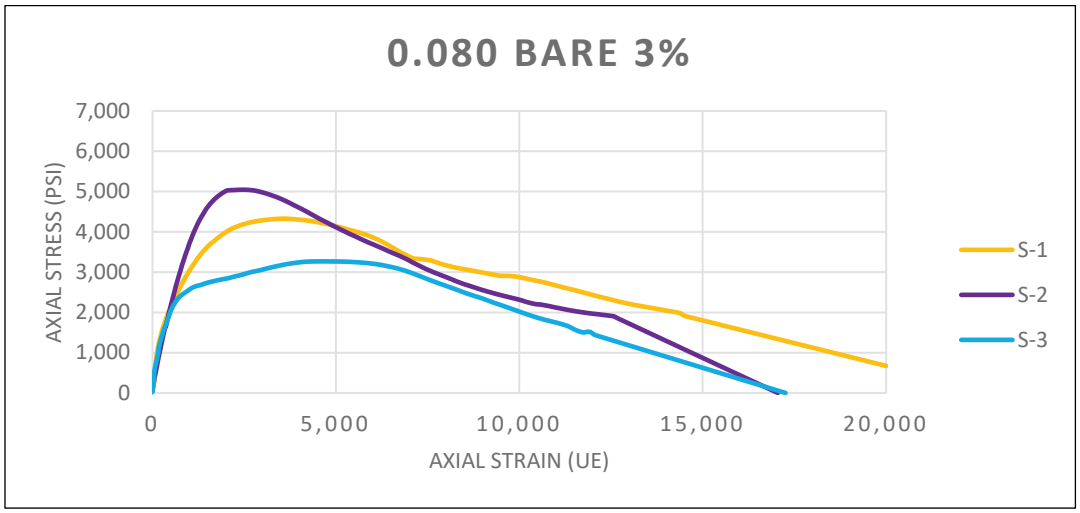

3.3.10 Set No. 10 – 0.047-in.-diam uncoated fibers (1% loading)

Cylinders with uncoated 0.047-in.-diam fibers (1% loading) before and after compression tests are shown in Figures 58 and 59, respectively. Figure 60 shows the compression stress-strain response of the specimens. During initial loading, the strain of the concrete increased with load in a linear manner, followed by a non-elastic response until the peak load was reached.

All three cylinders show a relatively similar pre-crack behavior, with Specimen 2 having a slightly higher compressive strength than the other two specimens. Specimen 1 had consolidation problems, and some of its area had concrete missing on the sides, which could possibly reduce the strength of the cylinder. The average compressive strength value for this set was 4,308 psi with a CV of 5.7%.

All three cylinders showed vertical cracks over their surfaces after testing. The post-peak behavior of the cylinders had some variability in ultimate strain values. Overall, this set had a relatively low ductility (Figure 60).

Figure 58. Cylinders made with uncoated 0.047-in.-diam fiber (1% loading) before testing.

Figure 59. Cylinders made with uncoated 0.047-in.-diam fiber (1% loading) after testing.

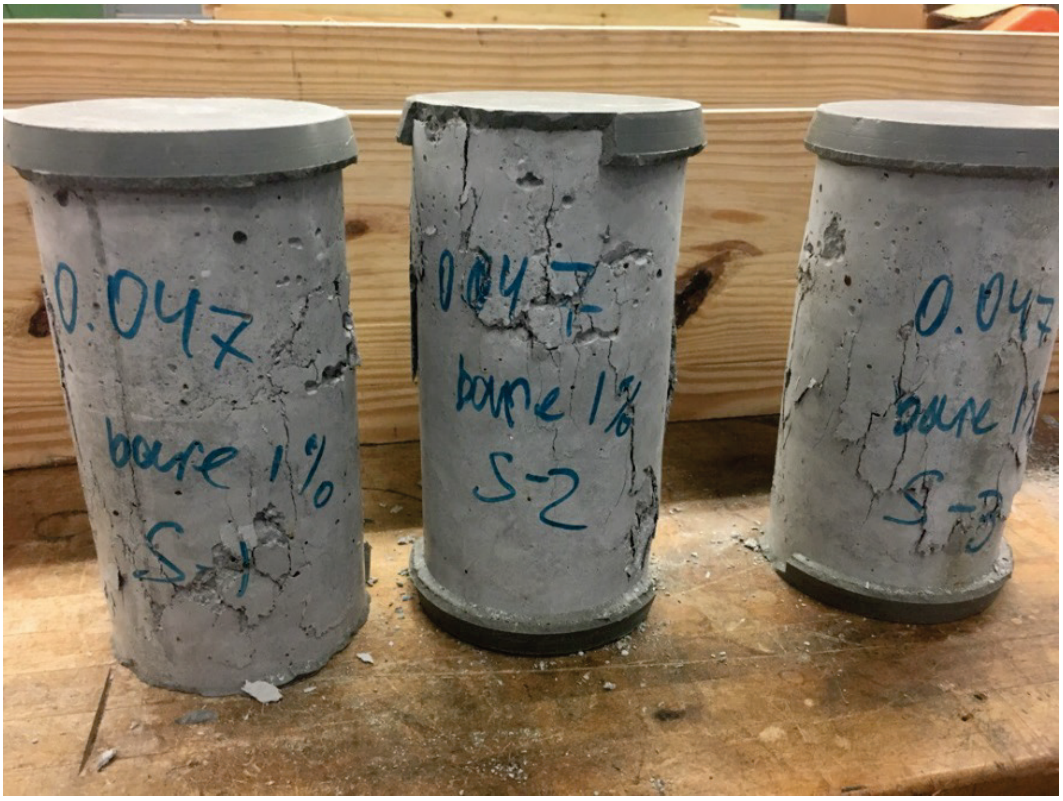

Figure 60. Compression stress-strain behavior of cylinders with uncoated 0.047-in.-diam fiber (1% loading).

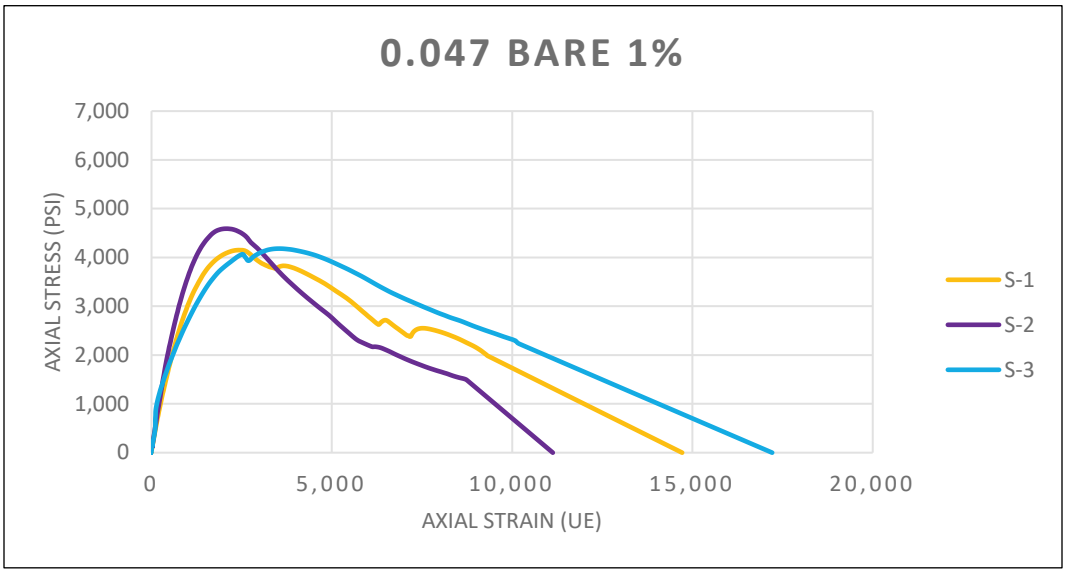

4 Masonry Test Results

4.1 Masonry prism compression results

The results of rectangular-prism compression tests for the masonry mixes are shown in Table 8. The age of specimens varied, but all specimens were more than two months old during testing. As is typical of proportion-based fine grout, the compressive strength of the control configuration of the grout (no fibers) was quite high and well above the minimum 2,000 psi required by the code (TMS 2016). The compressive strength of the grout also varied with fiber loading with the 0.047-in.-diam coated fiber appearing to increase the compressive strength of the grout at 1% loading but to decrease the compressive strength at 2% loading. Furthermore, the presence of the 0.029-in.-diam coated fibers appeared to decrease the compressive strength of the grout at 1% loading.

The typical grout prism failure, with significant vertical cracking shown on the surfaces, is shown in Figure 61.

Table 8. Grout compression test results.

Rectangular Prism Compression Tests Summary							
Configuration	Specimen No.	Width (in.)	Length (in.)	Height (in.)	Max Load (lb)	Max Stress (psi)	Average Stress (psi)
Control	1	3.00	3.00	6.78	55,300	6,144	5,744
	2	3.00	2.94	6.92	56,300	6,389	
	3	3.00	3.00	6.81	42,300	4,700	
0.029-in.-diam (1% loading)	1	3.44	3.50	6.50	58,500	4,862	5,007
	2	3.25	3.50	6.20	65,300	5,741	
	3	3.00	3.31	6.59	43,900	4,418	
0.047-in.-diam (1% loading)	1	3.28	3.29	6.92	75,500	6,982	6,666
	2	3.38	3.45	6.81	75,500	6,477	
	3	3.27	3.32	6.75	71,100	6,541	
0.047-in.-diam (2% loading)	1	3.38	3.44	6.78	56,900	4,905	4,058
	2	3.31	3.25	6.77	31,300	2,907	
	3	3.08	3.08	6.73	41,300	4,362	

Figure 61. Rectangular prism with coated 0.047-in.-diam fibers (1% loading) after testing.

4.2 Masonry wallet test results

4.2.1 Set No. 1 - control

Masonry wallet specimens with non-reinforced grout exhibited brittle failures. Control specimen 3 was tested by loading only one of the rebars, since the exposed rebar on one side of the right-hand bar splice was not long enough to provide sufficient load transfer through the rebar coupler. A control wallet specimen prior to testing is shown in Figure 62. All specimens were loaded beyond 36,000 lb (the specified yield load of the rebar) per rebar when the masonry surrounding one of the splices split suddenly. The typical wallet specimen after failure is shown in Figure 63. The load-deflection responses of all three control specimens are presented in Figure 64.

Figure 62. Plain (control) masonry wallet before testing.

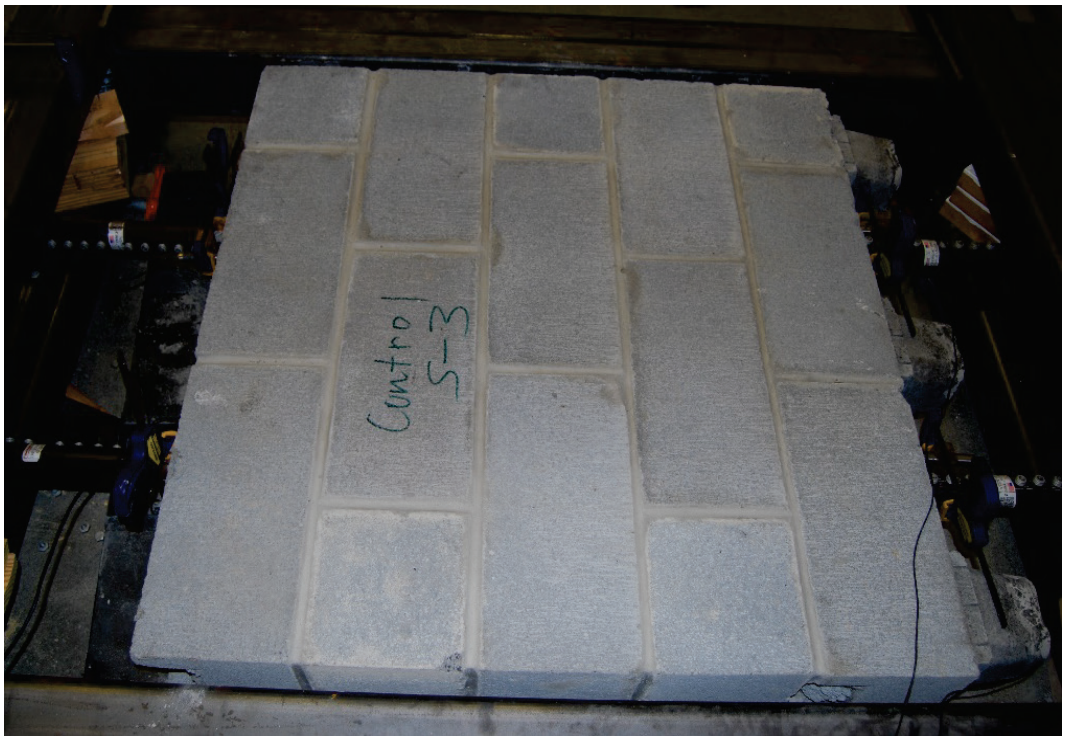

Figure 63. Plain (control) masonry wallet after failure.

Figure 64. Plain (control) masonry wallets' bar load-deflection response.

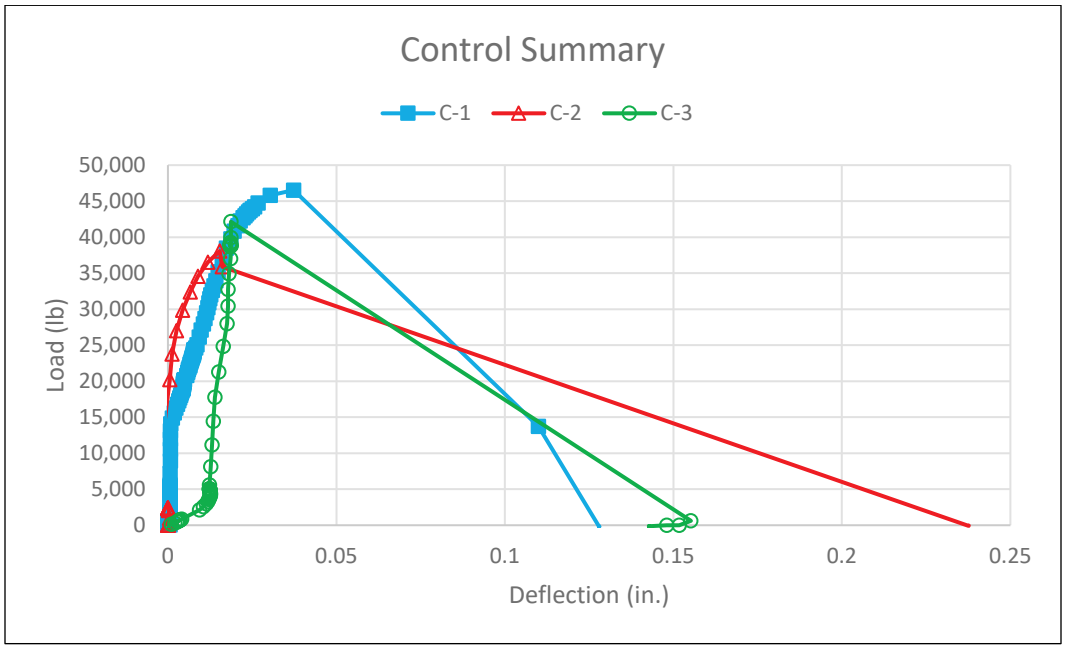

4.2.2 Set No. 2 - 0.029-in.-diam coated fiber (1% loading)

The masonry wallet specimens reinforced with 1% loading of the 0.029-in.-diam coated fibers showed very high ductility and much higher capacities than the control (Figure 65). Specimen 1 had to be retested because of issues with a loading frame; however, it still showed the highest peak bar load in the set. Average tested stress to 60 ksi (specified bar yield) stress ratio is 1.32, meaning the results significantly exceed the specified rebar yield load, well above the 1.25 required for rebar couplers by the Masonry Design standard (TMS 2016). Significant bar yielding in all three test specimens is shown in Figure 65.

The masonry wallet specimens' conditions after the tests are shown in Figure 66, Figure 67, and Figure 68. Both Specimens 1 and 3 showed very little sign of external cracking (only minor bed joint cracking), while Specimen 2 showed significant damage (probably caused by the obvious void exposed at midsplice in Figure 68). However, the capacity and ductility of all three specimens remained high.

Figure 65. Coated 0.029-in.-diam fiber (1% loading) masonry wallets bar load deflection response.

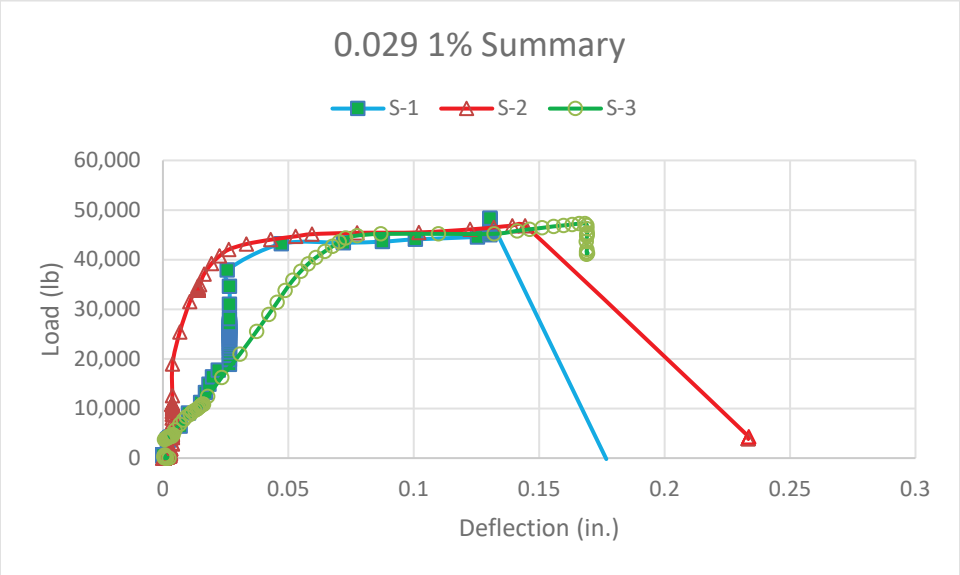

Figure 66. Coated 0.029-in.-diam fiber (1% loading) specimen S-1 after failure.

Figure 67. Coated 0.029-in.-diam fiber (1% loading) specimen S-3 after failure - no cracking.

Figure 68. Coated 0.029-in.-diam fiber (1% loading) specimen S-2 after failure, with an obvious void in the grouted cell.

4.2.3 Set No. 3 - 0.047-in.-diam coated fiber (1% loading)

The rebar load-deflection responses of masonry wallets reinforced with 1% of 0.047-in. coated fibers are shown in Figure 69. These specimens generally showed relatively high ductility, but lower peak bar loads compared to the control set. For Specimens 1 and 3, only one bar splice was tested, as the length of the exposed rebar on one of the specimen splices was not sufficient to allow the couplers to achieve full bar yielding (Figure 70). Specimen 3 failed prematurely due to this deficiency on the tested splice (rebar pulled out of the coupler). The average tested stress to the specified rebar yield stress (60 ksi) ratio was 1.10, and all three specimens appeared to indicate some yielding of the rebars. The minor cracking after failure of Specimen 1 is shown on Figure 71.

Figure 69. Coated 0.047-in.-diam fiber (1% loading) masonry wallet bar load deflection response.

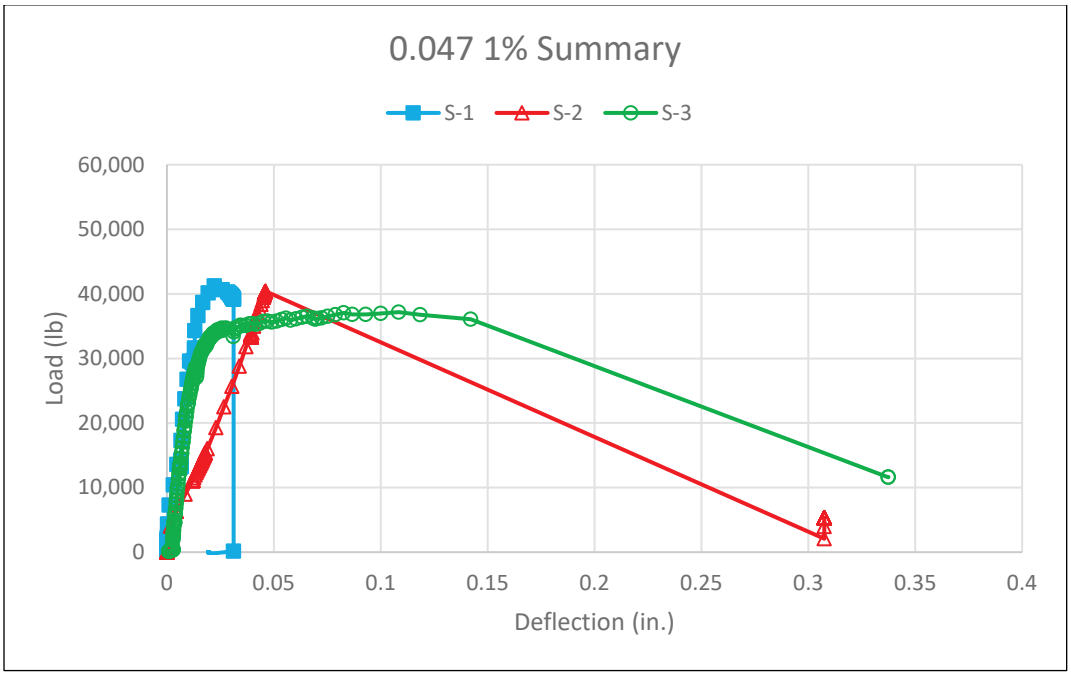

Figure 70. Short rebar end.

Figure 71. Coated 0.047-in.-diam fiber (1% loading) specimen S-1 cracking after failure.

4.2.1 Set No. 4 - 0.047-in.-diam coated fiber (2% loading)

The rebar load-deflection responses of masonry wallets reinforced with 2% of 0.047-in. coated fibers is shown in Figure 72. These wallets showed the highest ductility and highest tensile strength of the wallets tested. Minor cracking of the masonry wall was observed in Specimens 1 and 3 (Figure 73). However, Specimen 2 broke vertically all the way along the splice (Figure 74). Average tested stress to 60 ksi stress ratio is 1.34, meaning all three specimens significantly exceeded rebar yielding point and the Masonry Standard (TMS 2016) minimum of 1.25 for rebar couplers.

Figure 72. Coated 0.047-in.-diam fiber (2% loading) masonry wallet bar load-deflection response.

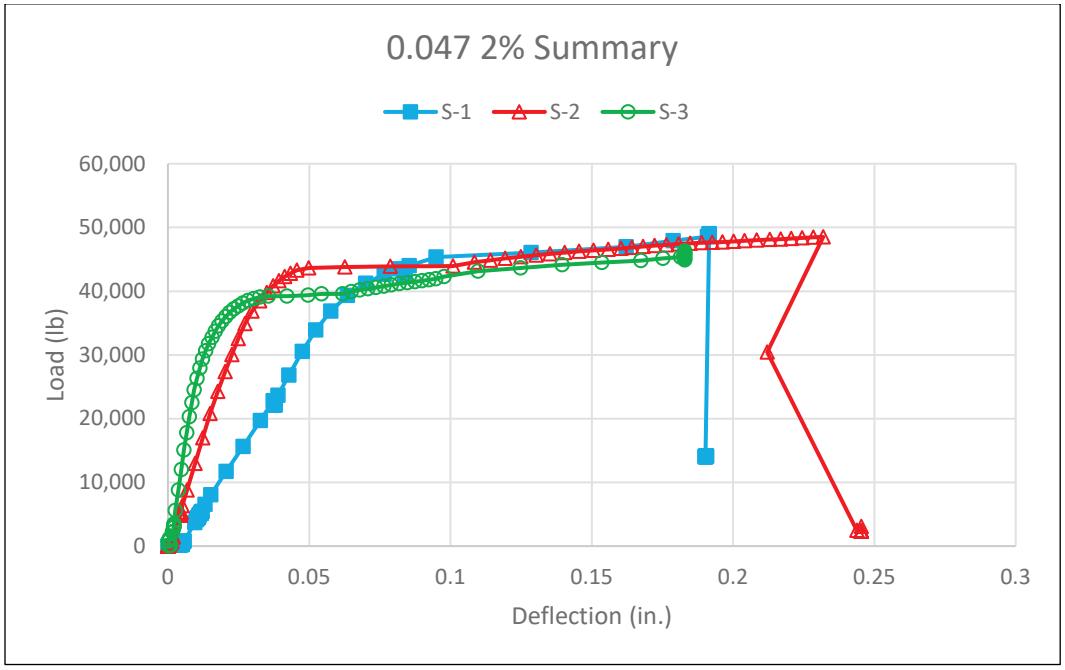

Figure 73. Coated 0.047-in.-diam fiber (2% loading) specimen S-3 after failure.

Figure 74. Coated 0.047-in.-diam fiber (2% loading) specimen S-2 after cracking.

4.2.2 Masonry wallet rebar pullout tests

A summary of the test results for all 12 masonry wallet rebar pullout tests is shown in Table 9. Representative loaded deflection responses for each set of wallet tests are shown in Figure 75. It is clear from the test results that use of coated steel fibers in the fine masonry grout can significantly increase the ductility of the steel rebar lap splices' tension load-deflection responses. Furthermore, addition of 1% (by volume) of 0.047-in.- diam coated steel fibers in the fine grout mix allowed the rebar to achieve yielding of the bars in two of the three bars tested and exceeded the specified yield strength of the rebar in all three tests.

Addition of 0.047-in.-diam coated fibers to the fine grout mix (at 2% by volume) allowed the rebar splice to be loaded past the 1.25 times the specified yield of the bars (60 ksi) required for mechanical connector for grade 60 rebar in the masonry design code (TMS 2016).

Addition of 0.029-in.-diam coated fibers (1% by volume) into the grout mix allowed the rebar splices to be tension loaded past the 1.25 times the specified yield of the bars (60 ksi) required for mechanical connector for grade 60 rebar in the masonry design code.

Table 9. Masonry wallet test summary.

Test Data Summary								
Configuration	Specimen No.	Date Cast	Date Tested	Max Load (lb)	Max Stress (psi)	$\sigma_{max}/_{60\ ksi}$	Average Stress (psi)	Average Ratio
Control	1	6/7/2018	10/15/18	46,538	77,393	1.29	70,269	1.17
	2	6/7/2018	10/15/18	38,081	63,328	1.06		
	3	6/7/2018	10/01/18	42,144	70,086	1.17		
0.029-in.-diam (1% loading)	1	6/7/2018	10/19/18	48,337	80,384	1.34	78,962	1.32
	2	6/7/2018	10/21/18	46,844	77,902	1.30		
	3	6/7/2018	10/22/18	47,264	78,601	1.31		
0.047-in.-diam (1% loading)	1	5/7/2018	10/01/18	41,233	68,571	1.14	65,861	1.10
	2	5/7/2018	09/29/18	40,404	67,193	1.12		
	3	5/7/2018	08/28/18	37,173	61,819	1.03		
0.047-in.-diam (2% loading)	1	5/7/2018	10/17/18	48,998	81,484	1.36	79,713	1.33
	2	5/7/2018	10/18/18	48,514	80,678	1.34		
	3	5/7/2018	10/19/18	46,287	76,975	1.28		

Figure 75. Masonry wallet test summary.

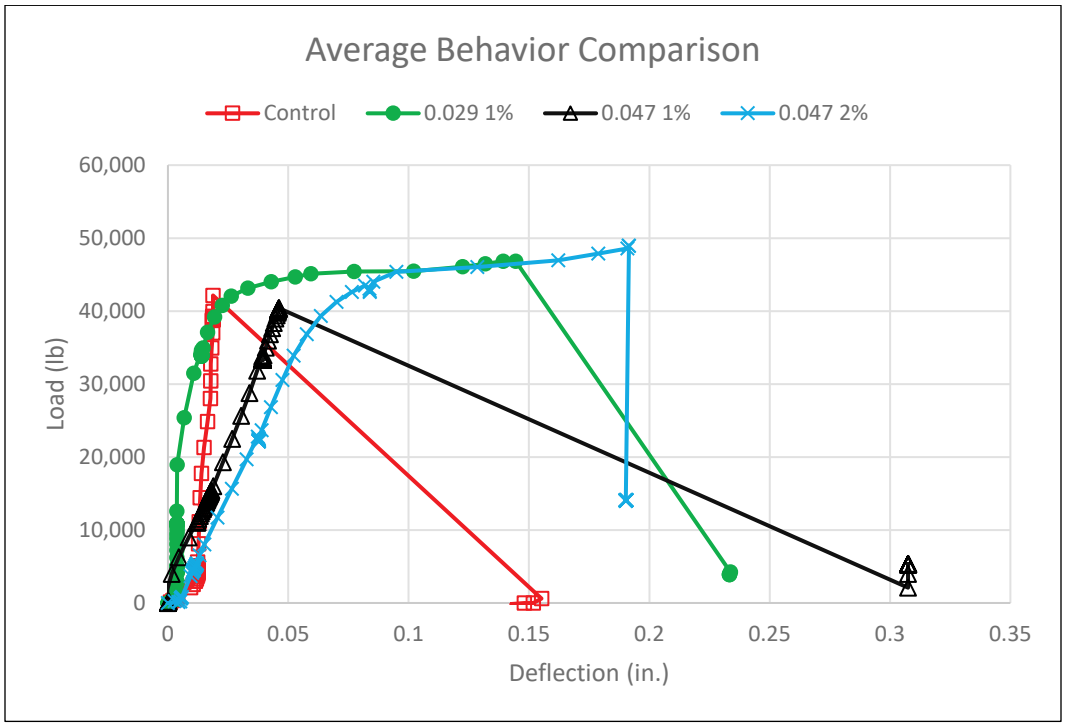

It is clear that coated steel fibers can be used to provide confinement of the masonry and rebar lap splices. With further testing to optimize the fiber configurations and test the splice capacity under dynamic loading over a wider range of rebars, use of fiber-reinforced grout may be shown to be a viable alternative to rebar couplers or confinement reinforcing in masonry wall systems. This could prove to be a significant savings in masonry construction, as lap splices of bars are costly, as are couplers and confinement bars.

5 UHPC Test Results

5.1 Flexural test results

Flexural testing was performed on beams with coated and uncoated fibers. Figures 76-79 show cross sections of beams after ASTM C1609 (2019b) testing. The light-colored areas of material that can be seen in some of the cross sections are agglomerations of silica fume that did not break up during mixing. This is common in UHPCs due to the high amounts of silica fume and the lack of coarse aggregate in the mixtures to break up agglomerations. The agglomerations were more predominant in the beams with larger fibers. This can most likely be attributed to typical variablility between concrete batches.

Figure 76. Cross section of uncoated 0.047-in.-diam fiber (1% loading) beam post testing.

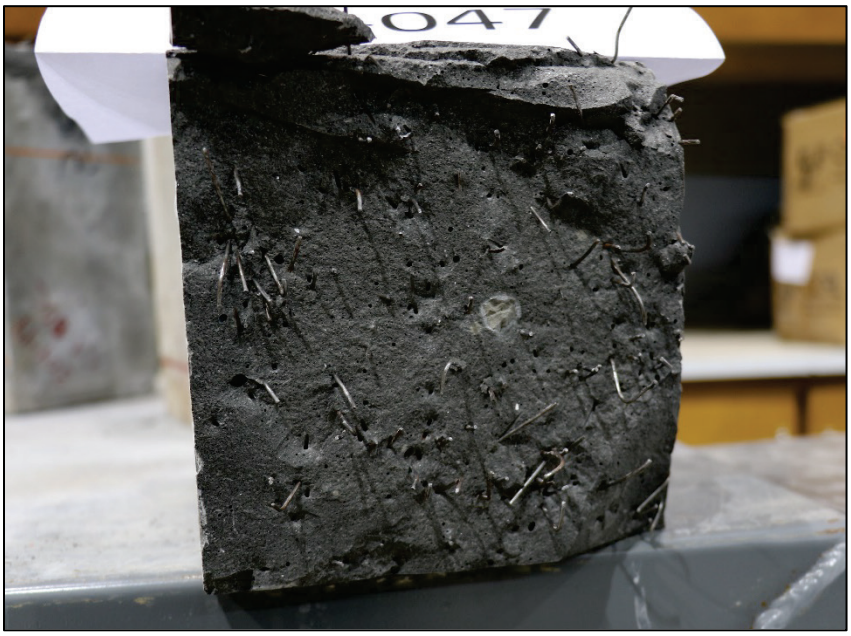

Figure 77. Cross section of uncoated 0.080-in.-diam fiber (1% loading) beam post testing.

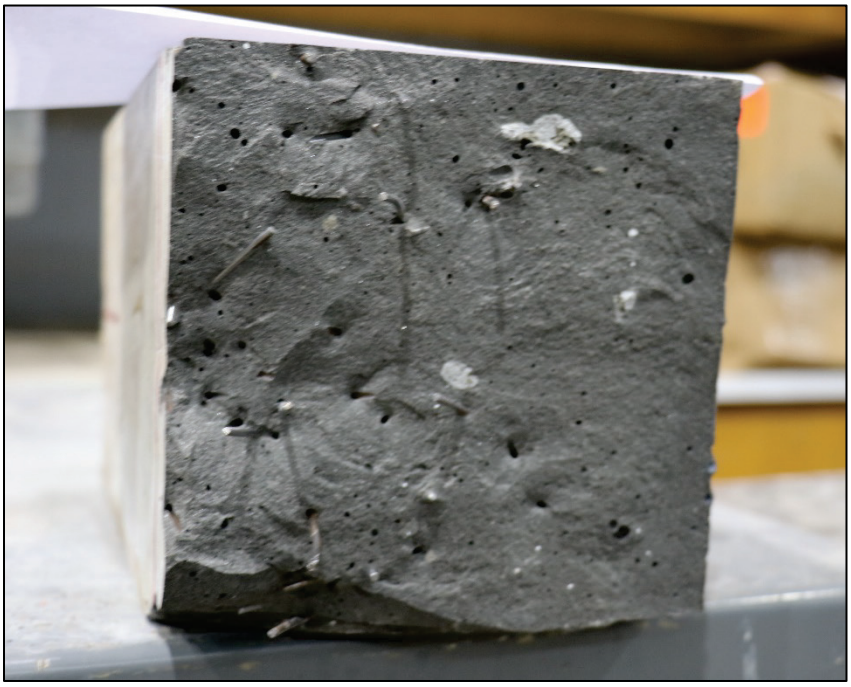

Figure 78. Cross section of coated 0.047-in.-diam fiber (1% loading) beam post testing.

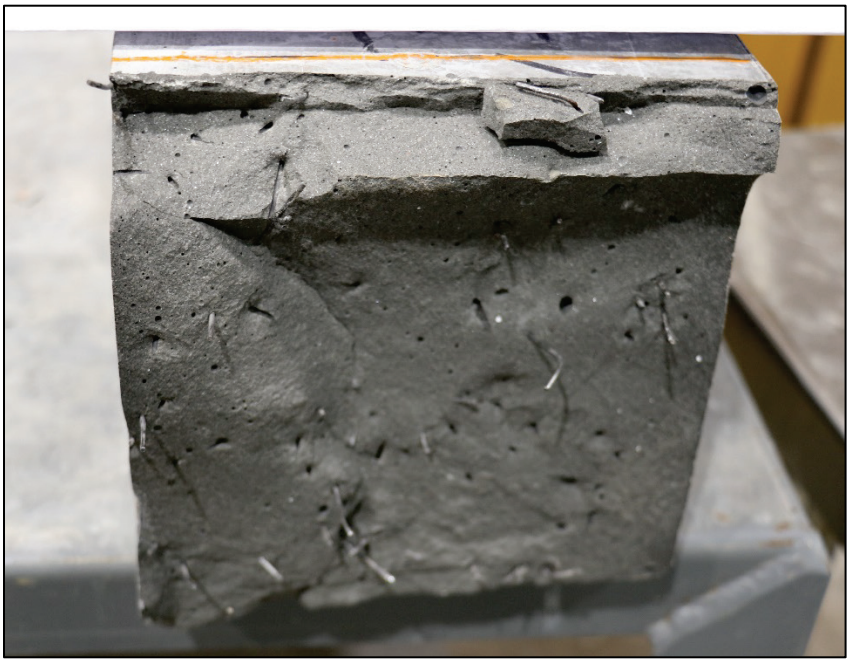

Figure 79. Cross section of coated 0.080-in.-diam fiber (1% loading) beam post testing.

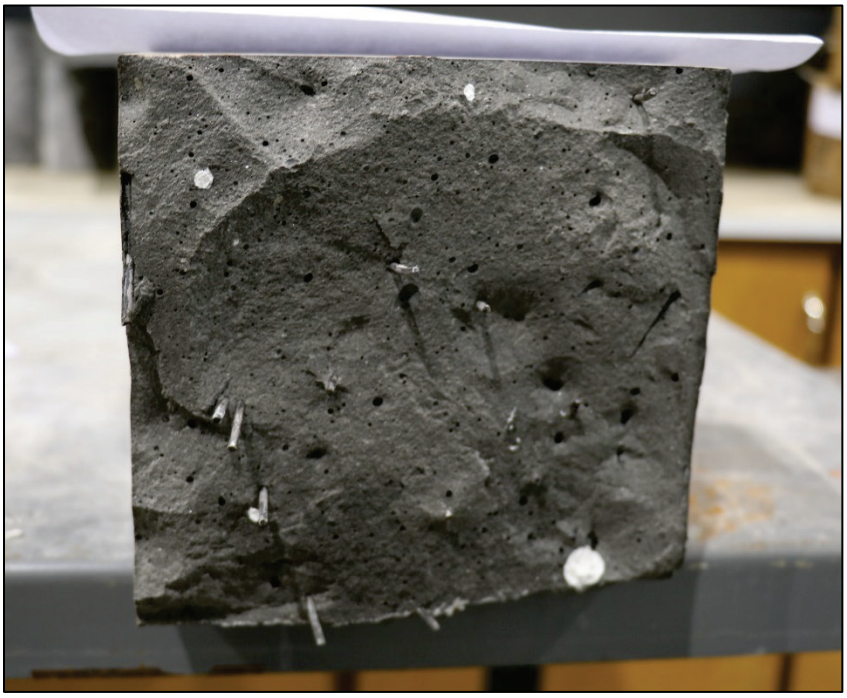

Figure 80 displays load versus deflection data from the ASTM C1609 (2019b) tests of the beams cast with uncoated fibers. The beams with 0.047-in.-diam fibers plotted in blue and green had higher peak strengths than the beams with 0.080-in.-diam fibers, and the curves decreased more gradually.

Figure 80. Load-deflection response of uncoated 0.080-in.-diam fiber (1% loading) and uncoated 0.047-in.-diam fiber (1% loading) UHPC beams.

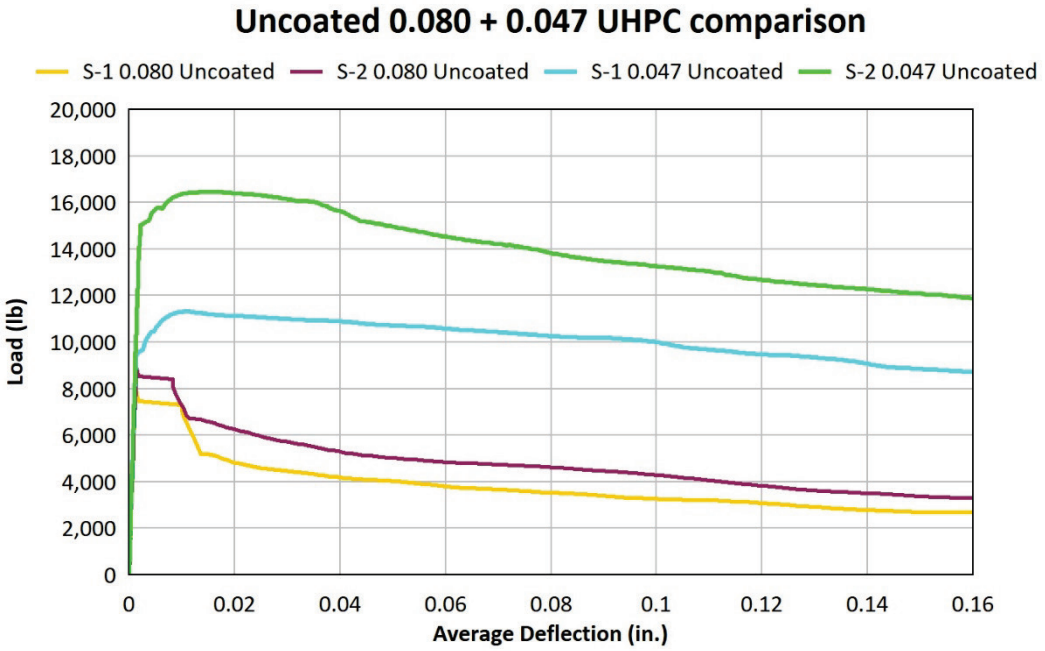

Figure 81 displays load versus deflection data from the ASTM C1609 (2019b) tests of the beams cast with coated fibers. Once again, the beams with 0.047-in.-diam fibers outperformed the beams with 0.080-in.-diam fibers.

Figure 81. Load-deflection response of coated 0.080-in.-diam fiber (1% loading) and coated 0.047-in.-diam fiber (1% loading) UHPC beams.

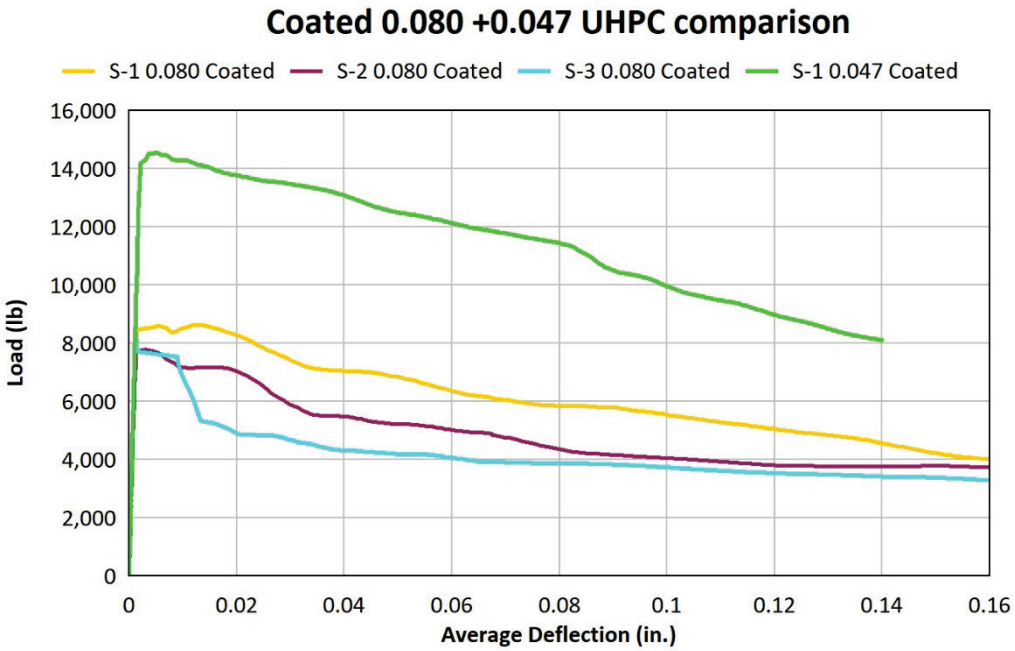

Table 10 summarizes the UHPC beam test results. There were errors with the LVDTs during some of the tests, hence the increased number of tests for modulus of rupture (MOR) results. Little difference was observed when comparing results for uncoated and coated 0.080-in.-diam fibers. This is most likely because there were not enough fibers in the mixture to significantly delocalize cracking. The coated 0.047-in.-diam fibers did perform significantly better than the uncoated fibers. The MOR for coated 0.047 in.-diam fibers was 50% higher than that of the uncoated fibers.

Overall, coated and uncoated fibers of the same thickness performed similarly. Thinner fibers performed better in UHPC than the thicker fibers. More individual fibers are required to achieve the desired volumetric fiber loading when thinner fibers are used. Mixtures with thinner fibers contain more fibers to bridge cracks and, therefore, perform better in flexure. The curves from the beams with thicker fibers also had sharper slopes post-failure. This shows that the beams with thinner fibers are a tougher material, as toughness can be described as the ability of a material to absorb energy.

Table 10. UHPC beam test results.

Fiber Type	MOR (psi)	Average MOR (psi)
0.080-in.-diam	930	900
	870	
0.080-in.-diam coated	880	812
	725	
	830	
0.047-in.-diam	1,370	1,505
	940	
	2,205	
0.047-in.-diam coated	2,695	2,263
	2,795	
	1,300	

5.2 Compression test results

The results for ASTM C39 (2015) testing at 28 days are shown in Table 11. The same water-cement ratio was used for all four mixtures so that the UCS of each should be similar. All four mixtures exceeded the 22,000-psi minimum for UHPC. Fiber content generally does not have much of an effect on pre-cracking UCS, but the coated fibers did

perform better than the uncoated fibers. The 0.047-in.-diam coated fibers had a 7% higher compressive strength than that of the uncoated fibers, whereas the 0.080-in.-diam coated fibers had a 19% higher compressive strength than that of the uncoated fibers.

Table 11. UHPC compression test results.

Fiber Type	Compressive Strength (psi)	Average Compressive Strength (psi)
0.047-in.-diam	35,170	29,765
	25,550	
0.047-in.-diam coated	28,575	31,885
	32,980	
	34,100	
0.080-in.-diam	27,295	25,912
	27,875	
	22,565	
0.080-in.-diam coated	31,580	30,943
	30,985	
	30,265	

Differences in UCS can be caused by batching errors, cylinder casting errors, or different fiber types. The mixtures with coated fibers performed better than the mixtures with uncoated fibers, and the mixtures with smaller fibers performed better than the mixtures with larger fibers. A larger ITZ could potentially cause a failure plane during high stress loading, leading to a lower compressive strength. A better bond across the ITZ might reduce this behavior.

5.3 Nanoindentation test results

The nanoindention tests measured elastic modulus across the ITZ of each specimen in five different regions. Each path was programmed so the indenter would probe the enamel coating on the sixth point, 25 μm from the start of the path. Figures 82 and 83 display the average elastic modulus across each path in the ITZ of the specimens with uncoated fibers. The indenter probed the enamel coating at 25 μm for the coated fibers and the UHPC matrix for uncoated fibers. The data points at 0-20 μm are representative of the steel fiber, and the data points greater than 25 μm are representative of the UHPC matrix.

Figure 82. Average elastic modulus across the ITZ of uncoated 0.047-in.-diam fiber UHPC.

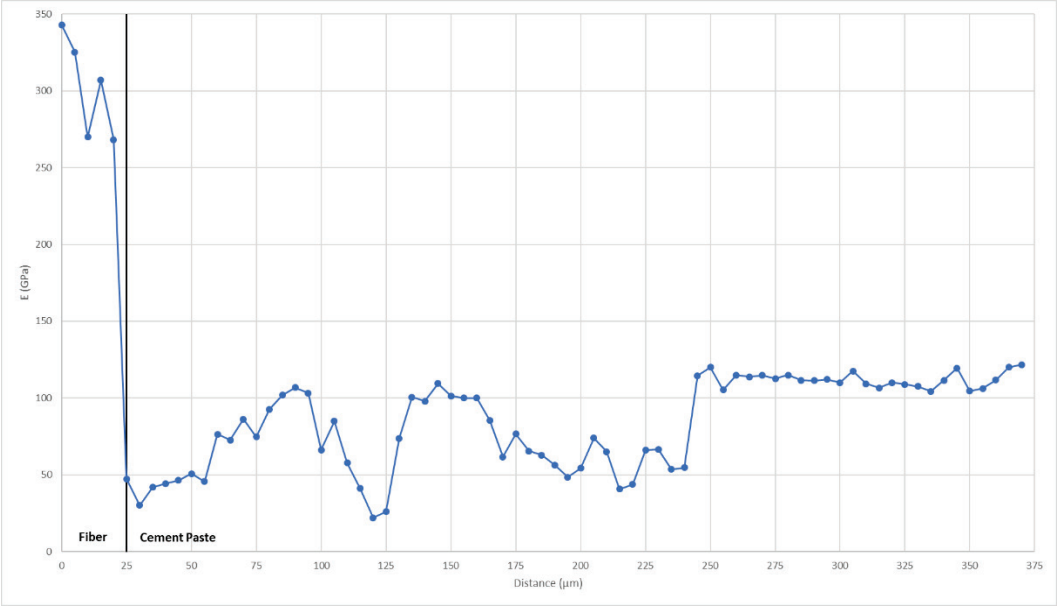

Figure 83. Average elastic modulus across the ITZ of uncoated 0.080-in.-diam fiber UHPC.

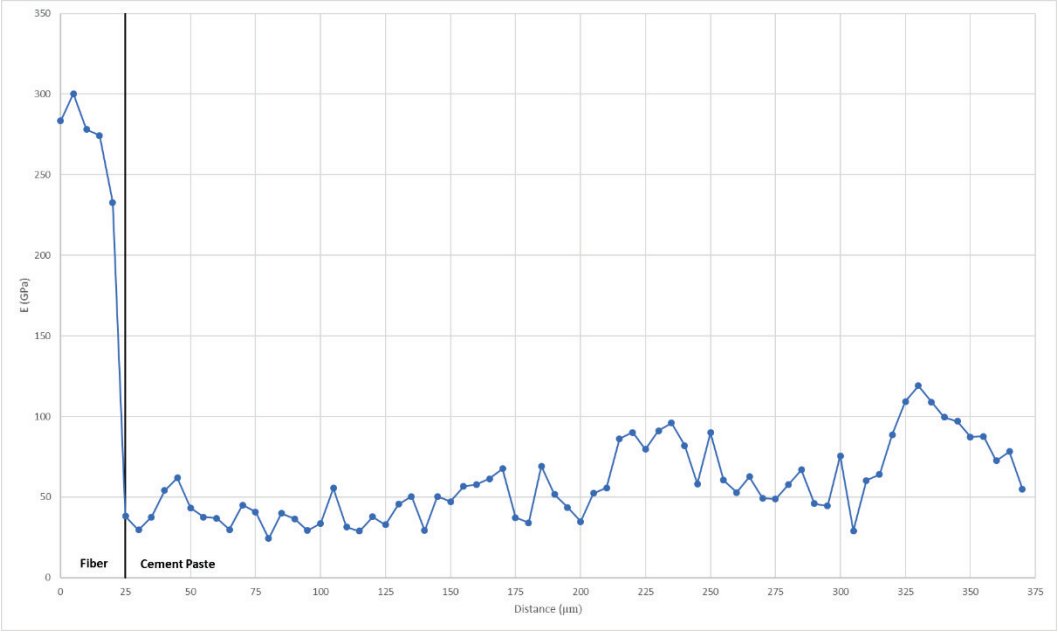

Figures 84 and 85 display the average elastic modulus across each path in the ITZ of the specimens' coated fibers. The enamel coating was probed at

25 µm. Data points at 0-20 µm are representative of the steel fiber, and the data points greater than 25 µm are representative of the UHPC matrix.

Figure 84. Average elastic modulus across the ITZ of coated 0.047-in.-diam fiber UHPC.

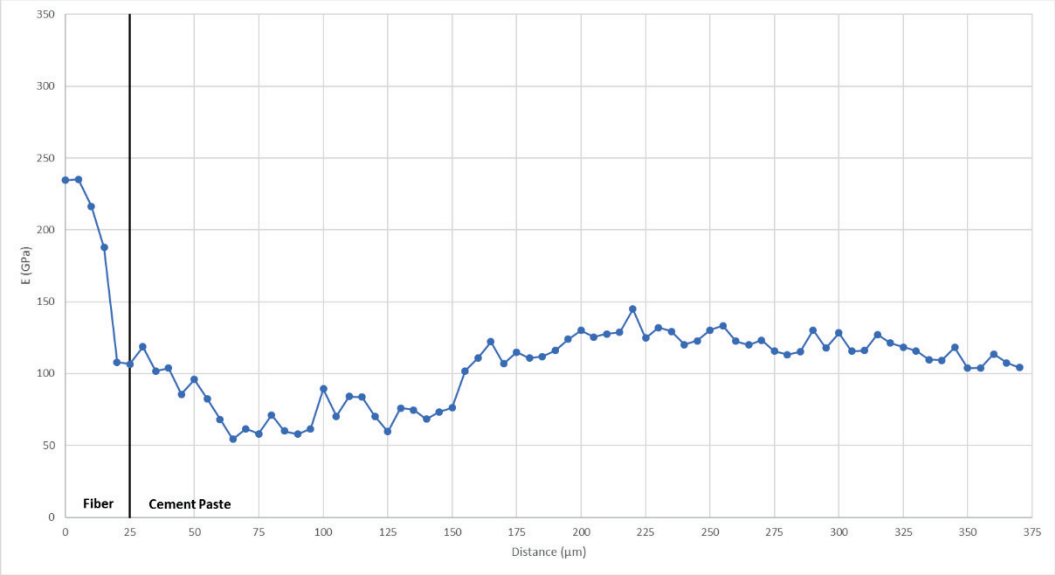

Figure 85. Average elastic modulus across the ITZ of coated 0.080-in.-diam fiber UHPC.

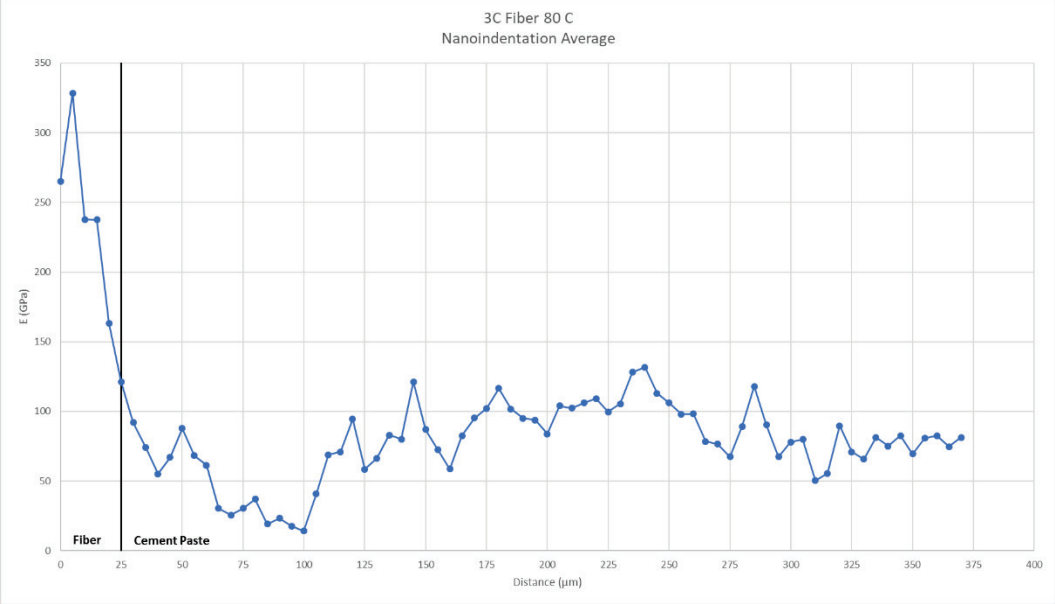

Figures 86 and 87 display load versus displacement for each material in the ITZ of the specimens with coated 0.047-in.-diam and 0.080-in.-diam fibers, respectively. These curves are representative of the maximum displacement exhibited by each material.

Figure 86. Load versus displacement of coated 0.047-in.-diam fiber UHPC materials.

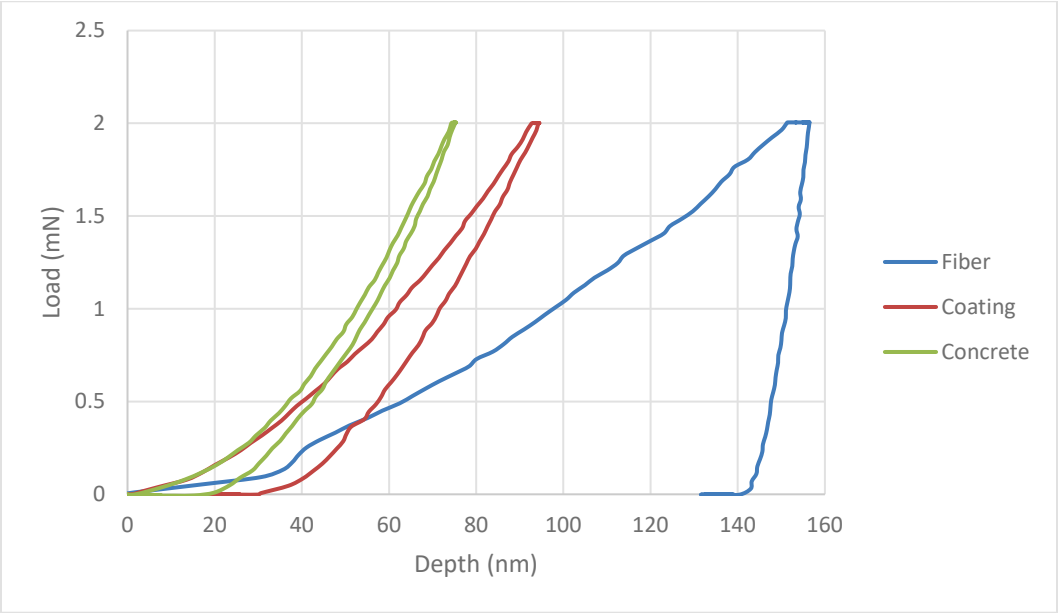

Figure 87. Load versus displacement of coated 0.080-in.-diam fiber UHPC materials.

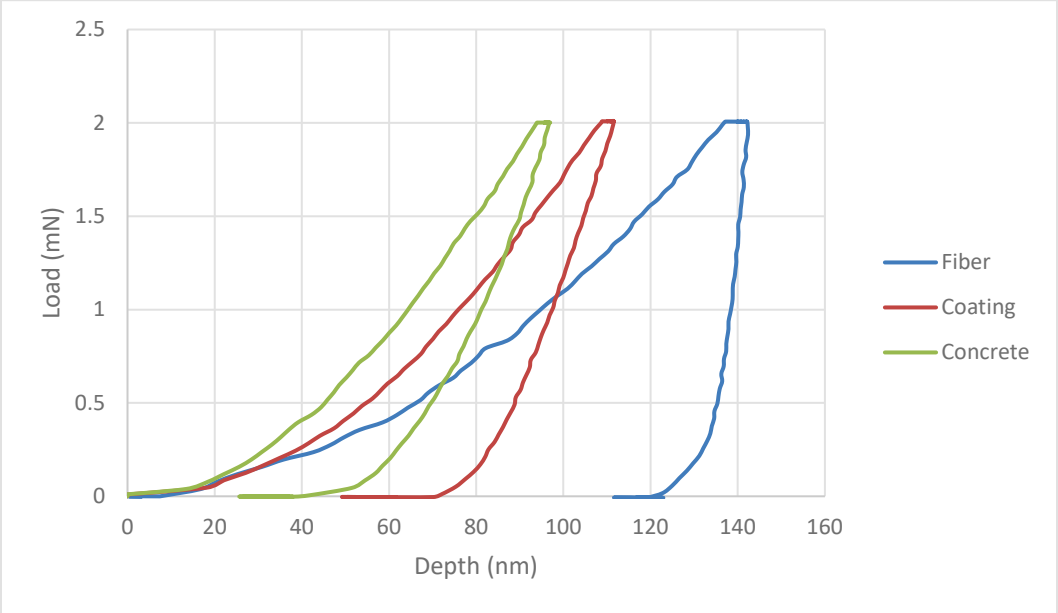

For both fiber types, the enamel coating exhibited a modulus between those of the UHPC matrix and the steel fiber. The coating serves as a transition point between the two materials. There is a gradual change in modulus across the ITZ in coated fibers compared to that of an uncoated fiber.

6 Discussion and Conclusions

6.1 Beam tests

Examination of Table 4 and the related load-deflection results allows the following observations and conclusions to be made.

1. A comparison of the MOR of the fiber-reinforced beams relative to the plain concrete beams showed an increase in cracking strength of 1.5 times for uncoated 0.080-in.-diam fibers to almost 3 times for the coated 0.080-in.-diam/0.047-in.-diam fiber mix.
2. Coated fibers showed a much higher MOR and ARS than uncoated fibers of the same volume loading, although the uncoated fiber mixes showed lower variations.
3. When comparing performances of two different fiber diameters, the mixture of 0.080-in.-diam and 0.047-in.-diam fiber mixes showed much higher strengths than the 0.080-in.-diam fiber mix. This appears to indicate that thinner fibers work better (produce greater increases in strength) in the concrete mix. A possible reason for this is the fact that the same concrete mix is more flowable with smaller diameter fibers. It is, therefore, easier for fibers to disperse throughout the mix, resulting in much better performance. Further investigation of this phenomenon is required, but this result suggests that coated fiber mixes with multiple diameters may improve fiber dispersions and effectiveness in the concrete mix.

6.2 Compression tests

Examination of Table 6 and the compression stress-strain responses of the fiber-reinforced concrete mixes allows the following observations and conclusions to be made.

1. Addition of both coated and uncoated fibers increased the ductility of the concrete compared to the same concrete with no fiber. Coated fibers appeared to provide significantly greater gains in ductility and strengths when compared to uncoated fibers, with the highest gains provided by the highest fiber percentage of the lowest diameter fibers.
2. Normally, the compressive strength of the concrete is reduced when fibers are added, but in this study the addition of 0.047-in.-diam. fiber

increased the compressive strength with peak gains achieved at fiber loads of 1% by volume.
3. Fiber volumes of 3% produced concrete mixes that were very difficult to consolidate and finish. Mixes with maximum fiber volumes less than 3% are recommended, at least for the fiber length and diameters investigated in this project.

6.3 Masonry wallet tests

Table 8 summarizes the test results for all 12 masonry wallet rebar pullout tests. Based on the results, the following observations and conclusions can be made.

1. Using coated-fiber reinforcement of fine masonry grout significantly increased the ductility of steel rebar lap splice load-deflection responses.
2. The addition (1% by volume) of 0.047-in.-diam coated fibers in a fine grout mix allowed the rebar to achieve measured yielding of the bars in all cases but one.
3. The addition (2% by volume) of 0.047-in.-diam coated fibers in the fine masonry grout mix allowed the No. 7 rebar lap splices to be loaded past the 1.25 x the specified yield of the bars (60 ksi) required for mechanical connector for grade-60 rebar in the masonry design code.
4. The addition of 1% by volume of 0.029-in.-diam coated fibers to the fine masonry grout mix allowed the No. 7 rebar lap splices to be loaded past the 1.25x the specified yield of the bars (60 ksi) required for mechanical connector for grade-60 rebar in the masonry design code.
5. Coated steel fiber reinforcing of fine masonry grout appeared to show great promise in confining steel rebar lap splices in masonry walls and may prove to be an economical alternative to long splices, confining bars, or mechanical couplers.

6.4 UHPC tests

Based on the results of the UHPC tests, the following observations and conclusions can be made.

1. The enamel coated 0.047-in.-diam fibers exhibited an MOR 50% higher than that of uncoated 0.047-in.-diam fibers at a 1% by volume dosage. The coated 0.080-in.-diam fibers did not demonstrate an increased performance compared to uncoated fibers. A higher dosage of fibers may better demonstrate the effect of the larger fiber.

2. The coated fibers performed better for unconfined compressive strength testing. The 0.047-in.-diam coated fibers exhibited a 7% increase in compressive strength, and 0.080-in.-diam coated fibers exhibited a 19% increase. The compressive strength of the mixtures with thinner fibers was higher than the compressive strength of those with thicker fibers.
3. Nanoindentation tests across the ITZ of coated and uncoated fibers showed a sharper transition in elastic modulus for specimens with uncoated fibers. The gradual transition in elastic modulus demonstrated by specimens with coated fibers is characteristic of a higher bond strength.

References

ACI (American Concrete Institute) Committee 318. 2014. *Building Code Requirements for Structural Concrete*. ACI 318-14. Farmington Hills, MI: ACI.

_____. 2018. *ACI concrete terminology*. ACI CT-18. Farmington Hills, MI: ACI.

ASTM (American Society for Testing and Materials International). 2014. *Standard test method for flexural strength of concrete (using simple beam with third-point loading)*. Designation: C78-14. West Conshohocken, PA: ASTM International. www.astm.org.

_____. 2015. *Standard test method for compressive strength of cylindrical concrete specimens* -- E-Learning Course. Designation: C39/C39M-15a. West Conshohocken, PA: ASTM International. www.astm.org.

_____. 2016a. *Standard specification for loadbearing concrete masonry units*: C90-16a. West Conshohocken, PA: ASTM International. www.astm.org.

_____. 2016b. *Standard test method for obtaining average residual-strength of fiber-reinforced concrete*. Designation: C1399/C1399M-16a. West Conshohocken, PA: ASTM International. www.astm.org.

_____. 2018a. *Standard practice for making and curing concrete test specimens in the laboratory*. Designation: C192/C192M-18. West Conshohocken, PA: ASTM International.

_____. 2018b. *Standard specification for grout for masonry*. Designation: C476-20. West Conshohocken, PA: ASTM International.

_____. 2019a. *Standard specification for mixing rooms, moist cabinets, moist rooms, and water storage tanks used in the testing of hydraulic cements and concrete.* Designation: C511-19. West Conshohocken, PA: ASTM International.

_____. 2019b. *Standard test method for flexural performance of fiber-reinforced concrete (using beam with third-point loading)*. Designation: C1609/1609M-19. West Conshohocken, PA: ASTM International.

Lui, Li. 2017. The macro-modelling of steel fiber reinforced concrete/mortar flexural tensile behavior and mix optimization for flexural strength. MS thesis, University of Louisville.

TMS (The Masonry Society). 2016. *Building code requirements for masonry structures and commentary*. TMS 402/602- 2016. Boulder, CO: The Masonry Society.

Unit Conversion Factors

Multiply	By	To Obtain
cubic feet	0.02831685	cubic meters
cubic inches	1.6387064 E-05	cubic meters
cubic yards	0.7645549	cubic meters
degrees Fahrenheit	(F-32)/1.8	degrees Celsius
feet	0.3048	meters
inches	0.0254	meters
pounds (force) per inch	175.1268	newtons per meter
pounds (force) per square inch	6.894757	kilopascals
pounds (mass)	0.45359237	kilograms
pounds (mass) per cubic foot	16.01846	kilograms per cubic meter
pounds (mass) per cubic inch	2.757990 E+04	kilograms per cubic meter
pounds (mass) per square foot	4.882428	kilograms per square meter
pounds (mass) per square yard	0.542492	kilograms per square meter
square feet	0.09290304	square meters
square inches	6.4516 E-04	square meters

REPORT DOCUMENTATION PAGE

Form Approved
OMB No. 0704-0188

1. REPORT DATE *(DD-MM-YYYY)*	2. REPORT TYPE	3. DATES COVERED *(From - To)*
May 2021	Final	

4. TITLE AND SUBTITLE

Performance of Active Porcelain Enamel Coated Fibers for Fiber-Reinforced Concrete:

The Performance of Active Porcelain Enamel Coatings for Fiber-Reinforced Concrete and Fiber Tests at the University of Louisville

5a. CONTRACT NUMBER
W912HZ-16-C-0015

5b. GRANT NUMBER

5c. PROGRAM ELEMENT NUMBER

6. AUTHOR(S)

Charles A. Weiss Jr., William M. McGinley, Bradford P. Songer, Madeline A. Kuchinski, and Frank A. Kuchinski

5d. PROJECT NUMBER

5e. TASK NUMBER

5f. WORK UNIT NUMBER

7. PERFORMING ORGANIZATION NAME(S) AND ADDRESS(ES)

Geotechnical and Structures Laboratory
U.S. Army Engineer Research and Development Center
3909 Halls Ferry Road
Vicksburg, MS 39180-6199

8. PERFORMING ORGANIZATION REPORT NUMBER

ERDC/GSL TR-21-15

9. SPONSORING / MONITORING AGENCY NAME(S) AND ADDRESS(ES)

U.S. Army Corps of Engineers
Washington, DC 20314-1000

10. SPONSOR/MONITOR'S ACRONYM(S)

11. SPONSOR/MONITOR'S REPORT NUMBER(S)

12. DISTRIBUTION / AVAILABILITY STATEMENT
Approved for public release; distribution is unlimited.

13. SUPPLEMENTARY NOTES

SBIR Phase II Sub-award Report Phase 2B

Small Business Innovation Research (SBIR) under Solicitation Number A14-090, "Highly Flexible Chopped Fiber Coating Apparatus," contract W912HZ-16-C-0015

14. ABSTRACT

A patented active porcelain enamel coating improves both the bond between the concrete and steel reinforcement as well as its corrosion resistance. A Small Business Innovation Research (SBIR) program to develop a commercial method for production of porcelain-coated fibers was developed in 2015. Market potential of this technology with its steel/concrete bond improvements and corrosion protection suggests that it can compete with other fiber reinforcing systems, with improvements in performance, durability, and cost, especially as compared to smooth fibers incorporated into concrete slabs and beams.

Preliminary testing in a Phase 1 SBIR investigation indicated that active ceramic coatings on small diameter wire significantly improved the bond between the wires and the concrete to the point that the wires achieved yield before pullout without affecting the strength of the wire.

As part of an SBIR Phase 2 effort, the University of Louisville under contract for Ceramics, Composites and Coatings Inc., proposed an investigation to evaluate active enamel-coated steel fibers in typical concrete applications and in masonry grouts in both tension and compression.

Evaluation of the effect of the incorporation of coated fibers into Ultra-High Performance Concrete (UHPC) was examined using flexural and compressive strength testing as well as through nanoindentation.

15. SUBJECT TERMS

Porcelain Enamel-coated fiber
Steel fiber
Fiber-Reinforced Concrete
Masonry wallet
Nanoindentation
Ultra-High Performance Concrete (UHPC)

16. SECURITY CLASSIFICATION OF:			17. LIMITATION OF ABSTRACT	18. NUMBER OF PAGES	19a. NAME OF RESPONSIBLE PERSON
a. REPORT	b. ABSTRACT	c. THIS PAGE			19b. TELEPHONE NUMBER *(include area code)*
Unclassified	Unclassified	Unclassified	SAR	88	